

## Analytical Techniques

Diffraction .....	2-40
Photoelectron Spectroscopy .....	41-54

(1) After solid-state products are obtained, quantitative and qualitative analysis must be carried out to obtain accurate chemical compositions and atomic structures. The most common analytical method used by solid-state chemists is X-ray powder diffraction (XPD), which can provide phase analysis and structural information for crystalline products. Single crystal diffraction will yield complete structural characterization. Complementary diffraction methods include neutron and electron diffraction, and there are numerous other techniques available such as nuclear magnetic resonance (NMR) and transmission electron microscopy (TEM), both of which also provide structural information. Chemical compositions can be determined by electron microscopy (SEM), microprobe analysis, X-ray fluorescence, X-ray photoelectron spectroscopy (XPS), inductively coupled plasma/mass spectrometry (ICP-MS), and via electrochemistry. Some of these techniques can help to assign oxidation states as well.

### Diffraction

READING: A.K. Cheetham and P. Day, Eds., *Solid-State Chemistry: Techniques*.

T. Proffen, R.B. Neder, S. Billinge, *Interactive Tutorial about Diffraction*,  
at <https://web.pa.msu.edu/cmp/billinge-group/teaching/teaching.html>

(2) Wavelengths and Energies: The distances between atoms in solids are on the order of 2–3 Å = 200–300 pm = 0.2–0.3 nm. Therefore, when atoms form periodic arrays in crystals, they can *diffract* light or matter waves that have wavelengths also on the order of 1 Å = 100 pm = 0.1 nm. Diffraction is the *coherent, elastic scattering* of radiation or matter waves. For crystalline solids, diffraction is accomplished by X-rays, neutrons, and electrons.

Two common sources of X-rays include Cu  $K\alpha$  radiation,  $\lambda = 1.54178 \text{ \AA} = 8.04 \text{ keV}$  ( $E = hc/\lambda$ ;  $hc = 12400 \text{ eV} \cdot \text{\AA}$ ); and Mo  $K\alpha$  radiation,  $\lambda = 0.71069 \text{ \AA}$ , 17.45 keV. The wavelength of  $K\alpha$  X-radiation decreases as atomic number  $Z$  increases according to Moseley's law,  $\lambda \propto Z^{-2}$ .

Neutrons were discovered for use in diffraction experiments around 1936 and require access to a nuclear reactor or spallation source for diffraction experiments. In this application, the wave nature of neutrons is obtained from de Broglie's relation:

$$\frac{1}{2}mv^2 = \frac{p^2}{2m} = \frac{1}{2m} \left(\frac{h}{\lambda}\right)^2 = \frac{3}{2}kT; \quad h = 6.63 \times 10^{-34} \text{ J}\cdot\text{sec} = 4.14 \times 10^{-15} \text{ eV}\cdot\text{sec};$$

$$k = 1.38 \times 10^{-23} \text{ J/K} = 8.61 \times 10^{-5} \text{ eV/K}.$$

The last part of this equation involves the equipartition principle, which relates the internal energy of a particle to its temperature via the Boltzmann relation. The rest mass of the neutron is  $m = 1.67 \times 10^{-27} \text{ kg}$ . For neutrons at a temperature of 298 K, the corresponding wavelength  $\lambda = 1.46 \text{ \AA}$ ,  $E = 38.5 \text{ meV}$  ( $v \sim 2700 \text{ m/sec}$ ). Such neutrons are called "thermal neutrons", and they can have larger effective neutron absorption cross-sections for nuclides than faster neutrons. A free neutron, i.e., one not part of an atomic nucleus, has an average lifetime of ca. 15 minutes by decaying to a proton + electron + antineutrino. This lifetime is long enough for scattering or diffraction experiments because thermal neutrons will spend just fractions of seconds traveling in the spectrometer from the source to the detector. Furthermore, for a given wavelength, neutrons have lower energies than X-rays, so radiation damage that can occur to a sample is significantly

reduced. However, neutron diffraction requires a large amount of material, a feature which is not always possible, whereas X-rays are effective for much smaller samples.

The matter waves of electrons are also described by de Broglie's relation using the rest mass of the electron ( $m = 9.11 \times 10^{-31}$  kg). For electrons to have a wavelength of  $1.50 \text{ \AA}$ , their energy must be  $\sim 70$  eV, and their speeds are  $\sim 5 \times 10^6$  m/sec =  $0.017c$ . For electron diffraction, however, electrons are typically accelerated by potentials of  $\sim 50$  keV, which means wavelengths of  $0.055 \text{ \AA}$  ( $55$  pm) and speeds of  $1.33 \times 10^8$  m/sec =  $0.443c$ . At these speeds, relativistic corrections are important. The smaller wavelengths associated with electron diffraction allow more information that can be gathered as compared to X-ray or neutron diffraction, but there are significant limitations as well: (a) sample thicknesses must be  $\sim 100$ nm or less to allow transmission of diffracted electrons; (b) at the energies involved, radiation damage is possible, especially if elemental components are volatile; (c) magnetic materials can deflect electrons by the Lorentz force, which makes structural determination especially challenging.

**(3) Producing X-rays – Conventional X-ray Tubes:** Light is generated by accelerating moving electrical charges or by inducing quantum transitions between energy states, although these two processes are equivalent. A conventional X-ray tube consists of a metal anode, e.g., Cu or Mo, which is bombarded by electrons generated from a tungsten coil and are accelerated across a voltage difference of ca. 50 kV. Characteristics of such X-ray tubes include (a) emission is isotropic, which implies that only a small fraction of all X-radiation emitted is actually used; (b) it is a single wavelength source; (c) the anode must be cooled, typically using water flow, because the high current used will melt the anode. Rotating the anode allows more power because the electron beam travels over the anode surface. *Rotating anode* sources offer greater intensities of X-radiation for diffraction, but frequently encounter mechanical problems.

**(4) When electrons hit the anode:** (a) they collide with atoms and decelerate, which leads to continuous radiation called *bremsstrahlung* or *white radiation*; and (b) they induce sharp transitions within the atom, producing X-rays of definite wavelengths called *characteristic radiation* by ionizing core orbitals following by relaxation. The two most intense transitions occur from the *L* and *M* shells to the *K* shell:



The bremsstrahlung radiation occurs above a minimum wavelength, or below a maximum energy, which is determined by the accelerating voltage ( $V$ ) of the electrons,  $\lambda_{\min} = (12.4 \text{ keV} \cdot \text{\AA})/V$ . This limit corresponds to the energy at which all kinetic energy of incident electrons is converted into X-rays. For the characteristic transitions, both  $K\alpha$  and  $K\beta$  radiation are doublets because of the two possible spin states associated with the  $p$  orbitals. On account of spin-orbit coupling, ionizing a closed shell  $p$  orbital will show  $p_{1/2}$  ( $l - s$ ) and  $p_{3/2}$  ( $l + s$ ) states. Examples of useful  $K\alpha$  and  $K\beta$  wavelengths (in  $\text{\AA}$ ) for X-ray diffraction are listed in the following table:

Anode Element	$K\alpha$ (average; $\text{\AA}$ )	$K\alpha_1$ ( $\text{\AA}$ )	$K\alpha_2$ ( $\text{\AA}$ )	$K\beta$ (average; $\text{\AA}$ )
Cr	2.29100	2.28970	2.29361	2.08487
Fe	1.93736	1.93604	1.93998	1.75661
Co	1.79026	1.78897	1.79285	1.62079
Cu	1.54184	1.54056	1.54439	1.39222
Mo	0.71073	0.70930	0.71359	0.63229

To achieve a monochromatic wavelength of the X-rays, they can be directed through a crystal *monochromator* and/or passed through a *filter*. Although both of these controls reduce the intensity of X-radiation, they are quite necessary to obtain a precise wavelength of the incident X-radiation so that accurate determination of unit cell parameters in solids can take place. One type of monochromator uses an oriented single crystal, e.g., Ge or SiO<sub>2</sub> single crystals, to focus X-rays passing through the sample and emerging at the detector. The principle uses the geometry of diffraction. On the other hand, filters rely on absorption, which follows Beer's law  $I = I_0 e^{-\mu d}$ , in which  $\mu$  = linear absorption coefficient and  $d$  = path length for X-rays to pass through the sample. The absorption coefficient  $\mu$  increases with wavelength (decreasing energy) according to  $\mu \sim A\lambda^3$ , but also shows discontinuities that correspond to absorption edges at wavelengths (energies) corresponding to the energy needed to eject an inner-shell electron – these *absorption edges* influence how a filter material should be selected. The goal of an X-ray filter is to allow  $K\alpha$  radiation through, but to block the higher energy  $K\beta$  characteristic energy, as well as much of the white radiation. As an example, the energy required to ionize the 1s electrons of Ni has a wavelength  $\lambda = 1.488 \text{ \AA}$ , which lies intermediate between Cu  $K\alpha$  and  $K\beta$  wavelengths. Thus, Ni is an effective filter for Cu sources. In general, a filter for element  $Z$  would be element  $Z-1$  or  $Z-2$ ; e.g., a Ni filter for Cu, a Zr filter for Mo.

**Notation:** Single-electron atomic levels and electronic transitions between levels use two related nomenclatures: (1) Spectroscopic notation, developed by chemists; and (2) X-ray (Siegbahn) notation, developed by physicists. Spectroscopic notation designates the atomic orbital with the subscript  $j = l \pm 1/2$  for orbitals with  $l \geq 1$  ( $p, d, f, \dots$ ). X-ray notation uses the capital letters  $K, L, M, N, O, \dots$  corresponding to the electronic shells with principal quantum numbers  $n = 1, 2, 3, 4, 5, \dots$ , respectively. Levels within each shell are designated by numerical subscripts that increase as the energy of the level increases. For example, the  $L$ -shell contains the three levels  $L_1(2s), L_2(2p_{1/2}),$  and  $L_3(2p_{3/2})$ .

Allowed electronic transitions between levels require  $\Delta l = \pm 1$ , such as  $2p_{1/2} \rightarrow 1s$ . In the X-ray convention, transitions are symbolized as either (i) two successive levels with the final level preceding the initial level or (ii) the final level designation followed by a Greek letter  $\alpha$  or  $\beta$ , corresponding to the change in shell number  $\Delta n = 1$  or 2. Numerical subscripts indicate relative intensities (degeneracies) of transitions between shells with 1 being the most intense. In the example,  $2p_{1/2} \rightarrow 1s \equiv KL_2 \equiv K\alpha_2$ . Here are the symbols for the atomic levels in shells 1 and 2 and allowed transitions that emit electromagnetic radiation:

$n$	$l$	$j$	Spectroscopic Symbol (Degeneracy)	X-ray Symbol
1	0	0	1s (2)	$K$
2	0	0	2s (2)	$L_1$
2	1	1/2	$2p_{1/2}$ (2)	$L_2$
2	1	3/2	$2p_{3/2}$ (4)	$L_3$

Allowed Transitions	
Spectroscopic Notation	X-ray Notation
$2p_{1/2} \rightarrow 1s$	$K\alpha_2$
$2p_{3/2} \rightarrow 1s$	$K\alpha_1$

**(5) Producing X-rays – Synchrotron Radiation:** Another way to accelerate electrons is to keep them moving in a circular fashion, which is the principle behind a *synchrotron*. Bending magnets continuously accelerate (deflect) a high energy electron beam. The radiation emitted is intense (possibly 5-8 orders of magnitude more intense than standard X-ray tubes), continuous (tunable), intrinsically collimated, pulsed, and polarized. However, synchrotrons require large-scale facilities, infrastructure, supervision, and maintenance. Moreover, the intensity of X-rays can incur radiation damage on the sample, and heating of optical elements. The Advanced Photon Source (APS) at Argonne National Laboratories is a synchrotron with radius of  $R = 175 \text{ m}$  (1100

m circumference) and electron kinetic energies of  $E = 7$  GeV. At these energies, each electron moves nearly at the speed of light, and radiates 52.9 nanowatts. The energy lost per revolution is 1.9 picojoules/electron ( $\sim 1.2$  MeV/electron). To replenish this lost energy from emission, the electrons move in radio frequency cavities, which provide

electric fields to keep the electrons at constant energy. The distribution of synchrotron radiation is continuous extending from the X-ray to the infrared region and is characterized by a critical wavelength  $\lambda_c$  (Å), which is 2.85 Å for the APS. This critical wavelength divides the radiated flux into parts of equal radiated power above and below this wavelength value.<sup>1</sup>

When using a synchrotron, there are numerous applications available that extend beyond diffraction. Some of these include: (i) spectroscopic information, e.g., EXAFS (Extended X-ray Absorption Fine Structure) and XANES (X-ray Absorption Near Edge Spectroscopy), which can give oxidation states and coordination numbers (not usually local geometry, though); (ii) very fast crystallography so as to access time-resolved phenomena, such as crystal dehydration or solid-solid phase transitions; (iii) obtaining high resolution and diffuse (background) scattering using small samples, experiments which provide intermediate correlated length scales in solids; (iv) magnetic scattering because of high energy radiation and the effect of local magnetic moments on some core electron energy states, e.g., in Gd compounds; and (v) higher wavelength radiation can undergo inelastic scattering, which provides information about local site potential energies and vibrational energies.

**(6) Producing Neutrons:** Neutrons are produced by fission of  $^{235}\text{U}$  in nuclear reactors or using spallation sources. Thermal neutrons are necessary to maintain the chain reaction; the product neutrons must be slowed, by passing them through a moderating medium, which is often  $\text{D}_2\text{O}$ . Spallation sources involve bombarding metal targets such as U, W, or Pb, with 800 MeV protons or GeV photons, which generate pulsed neutrons that are analyzed by *time-of-flight* methods. Both sources create a broad spectral Maxwell-Boltzmann distribution of wavelengths. At 300 K, the most probable wavelength is 1.78 Å. Time-of-flight methods allow for a distribution of wavelengths because the kinetic energy per neutron is inversely related to  $\lambda^2$  and directly related to speed squared  $= (D/t)^2$ , in which  $D$  = distance traversed by a neutron and  $t$  = time needed to traverse the distance. Thus,  $\lambda \propto t$ , the *time-of-flight*. This method is practical for diffraction using thermal neutrons ( $T \sim 300$  K), which have speeds  $\sim 10^5$  cm/sec and wavelengths of 1.3–2.5 Å. In the Bragg equation for diffraction between parallel planes of atoms separated by a distance  $d$  in a crystal, i.e.,  $\lambda = 2d \sin \theta$ , the wavelength of neutron matter waves will be variable. Therefore, detectors are placed at fixed angles  $\theta$  with respect to the incident beam of neutrons, and the distribution of  $\lambda$  allows measurement of various  $d$ -spacings in the solid.

**(7) Atomic Scattering – X-rays:** Diffraction is a *scattering* process that involves incident radiation traveling along a specific direction and interacting with the target specimen, which then scatters radiation in all directions. The scattered radiation is detected and analyzed for its scattered directions and intensities. An important parameter of scattering experiments is the cross section

**Important Features of Synchrotron Radiation:**

$$\text{Average Power Radiated / } e^- \text{ (nW)} = 674.4 \frac{E(\text{GeV})^4}{R(\text{m})^2}$$

$$\text{Energy Loss per Revolution / } e^- \text{ (keV)} = 88.46 \frac{E(\text{GeV})^4}{R(\text{m})}$$

$$\text{Critical Wavelength (Å)} = 5.59 \frac{R(\text{m})}{E(\text{GeV})^3}$$

<sup>1</sup> A. Balerna, S. Mobilio, in *Synchrotron Radiation: Basics, Methods, and Applications*, Eds. S. Mobilio, F. Boscherini, C. Meneghini, Springer, 2015.

$\sigma$ , which is essentially the contact area for scattering to occur; the unit is 1 barn =  $10^{-28}$  m<sup>2</sup>. The scattering efficiency along a particular direction is the *differential scattering cross section*  $d\sigma/d\Omega$ , in which  $d\Omega = dA/R^2$  ( $dA$  = area;  $R$  = distance between detector and target) is the infinitesimal solid angle for the scattered species. Since radiation is either electromagnetic or matter waves, the incident and scattered waves are  $\psi_0$  and  $\psi_s$  and the differential scattering cross section is:

$$\frac{d\sigma}{d\Omega} = \frac{\Phi_s}{\Phi_0} \cdot \frac{dA}{d\Omega} = \frac{|\psi_s|^2}{|\psi_0|^2} R^2 = \frac{I_s}{I_0} R^2.$$

$I_0$  and  $I_s$  are the corresponding intensities;  $\Phi_0$  and  $\Phi_s$  are the incident and scattered fluxes. The nature of the atomic scattering process differs between X-rays and neutrons: X-rays are scattered by electrons in atoms, whereas neutrons are scattered primarily by the nuclei of atoms.

Let's first consider X-ray scattering by a *single electron*. X-rays are electromagnetic waves described by oscillating electric and magnetic fields in mutually perpendicular planes as well as perpendicular to the direction of wave propagation, which is specified by the wavevector  $\mathbf{k}$ . The incident X-rays are represented as plane waves  $\psi_0 = \mathbf{E}_0 e^{-i\omega t} e^{i\mathbf{k}_i \cdot \mathbf{z}}$  with wavevector along the z-direction,  $\mathbf{k}_i = (2\pi/\lambda)\hat{\mathbf{z}}$ , energy  $\hbar\omega = hc/\lambda$ , and amplitude  $\mathbf{E}_0$  (this is the electric field magnitude). In the oscillating electric field of the X-radiation, the electron will oscillate (accelerate) and become a source of radiation scattered elastically in all directions as spherical waves. The acceleration of a single electron caused by the oscillating field  $\mathbf{E}_0$  of a single (polarized) X-ray is force/mass or  $\mathbf{a} = -e\mathbf{E}_0/m$ . The resulting scattered wave along the direction  $\mathbf{k}_s = (2\pi/\lambda)\hat{\mathbf{r}}$ , which is at an angle  $2\theta$  with respect to the incident ray  $\mathbf{k}_i$ , is:

$$\psi_s(r, 2\theta) = \frac{-(r_0 \cos 2\theta)}{r} \mathbf{E}_0 e^{-i\omega t} e^{i\mathbf{k}_s \cdot \mathbf{r}},$$

in which  $r_0 = e^2/mc^2 = 2.82$  fm = Thomson scattering length or classical radius of the electron and the negative sign arises from the negative sign of the electron acceleration. The difference between the incident and scattered wavevectors  $\mathbf{k}_i$  and  $\mathbf{k}_s$  is the *scattering vector*  $\mathbf{q} = \mathbf{k}_s - \mathbf{k}_i$ . The magnitudes of  $\mathbf{k}_i$  and  $\mathbf{k}_s$  are equal, so this is elastic scattering. By geometrical analysis of the isosceles triangle formed by the vectors  $\mathbf{k}_i$ ,  $\mathbf{k}_s$ , and  $\mathbf{q}$ , the length of the scattering vector is

$$q = (4\pi \sin \theta)/\lambda.$$

Wavevectors and scattering vectors have units of 1/length ("reciprocal" length), e.g., cm<sup>-1</sup>.

In usual diffraction experiments, the incident X-ray beam is unpolarized, which means that the field oscillation can occur in any direction with respect to the plane formed by the incident and scattered waves, given by the wavevectors  $\mathbf{k}_i$  and  $\mathbf{k}_s$ . Using geometrical optics, the incident and scattered waves have amplitudes and corresponding intensities both perpendicular and parallel to this plane:

$$\text{Incident waves:} \quad I_0 = I_{0\perp} + I_{0\parallel} \text{ with } I_{0\perp} = I_{0\parallel} = \frac{1}{2} I_0.$$

$$\text{Scattered waves:} \quad I_s = I_{s\perp} + I_{s\parallel} \text{ with } I_{s\perp} = \frac{I_0 r_0^2}{2 r^2}; \quad I_{s\parallel} = \frac{I_0 r_0^2}{2 r^2} \cos^2 2\theta, \text{ so that}$$

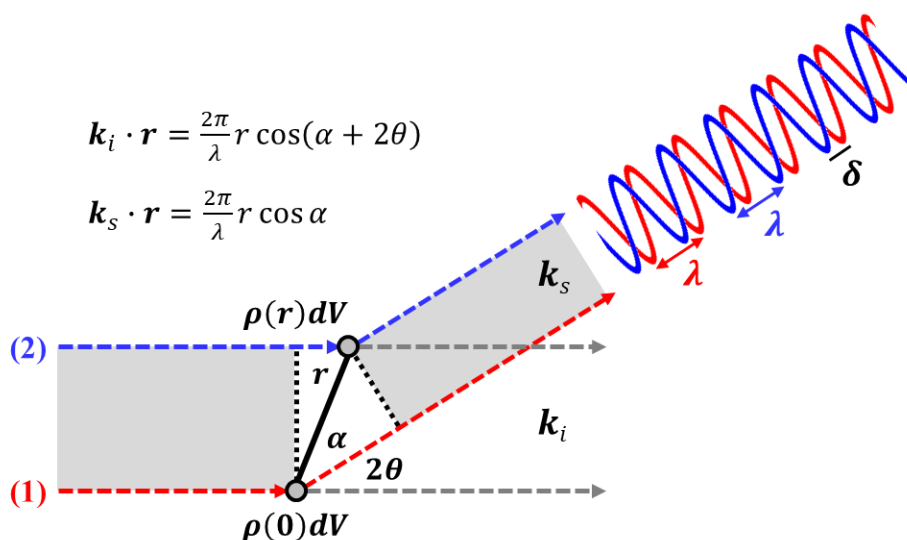
$$I_s = I_{s\perp} + I_{s\parallel} = I_0 \frac{r_0^2}{r^2} \left[ \frac{(1 + \cos^2 2\theta)}{2} \right] = \frac{I_0}{r^2} r_0^2 P(2\theta).$$

Therefore, the intensity of the scattered radiation is reduced relative to the incident beam by a *polarization factor*  $P(2\theta)$  and the scattering amplitude for one electron is  $A_s^{(e)} = -r_0 P^{1/2}(2\theta)$ . As a result, the scattered wave by one electron for unpolarized incident X-rays is

$$\psi_s(r, 2\theta) = \frac{-(r_0 P^{1/2}(2\theta))}{r} \mathbf{E}_0 e^{-i\omega t} e^{i\mathbf{k}_s \cdot \mathbf{r}} = \frac{A_s^{(e)}}{r} \mathbf{E}_0 e^{-i\omega t} e^{i\mathbf{k}_s \cdot \mathbf{r}}.$$

Also, since  $I_s/I_0 = (r_0/r)^2 P(2\theta)$ , if a detector is 10 cm from the sample, then each electron in the sample scatters no more than  $8 \times 10^{-28}$  of the incident radiation intensity.

(8) Next, consider X-ray scattering by two small negative charges  $\rho(\mathbf{0})dV$  and  $\rho(\mathbf{r})dV$  separated by a vector  $\mathbf{r}$ ;  $\rho(\mathbf{r})$  is the electron density at point  $\mathbf{r}$ . Each charge will scatter X-rays, and the resulting scattered ray at angle  $2\theta$  is a superposition of the two scattered waves. These scattered waves have a phase difference  $\varphi(2\theta)$  related to the path difference  $\delta(2\theta)$  the two waves travel and depends on the scattering angle  $2\theta$ :  $\varphi(2\theta)/2\pi = \delta(2\theta)/\lambda$ .



$$\mathbf{k}_i \cdot \mathbf{r} = \frac{2\pi}{\lambda} r \cos(\alpha + 2\theta)$$

$$\mathbf{k}_s \cdot \mathbf{r} = \frac{2\pi}{\lambda} r \cos \alpha$$

In this construction, rays (1) and (2) are in phase. Ray (1) is scattered by the charge at the origin; ray (2) is scattered by the charge at  $\mathbf{r}$ . The parts of the rays that are highlighted by the shaded region have equal lengths. Then, the path difference between the two rays is:

$$\delta(2\theta) = D(1) - D(2) = r \cos \alpha - r \sin\left(\frac{\pi}{2} - (\alpha + 2\theta)\right) = r \cos \alpha - r \cos(\alpha + 2\theta)$$

$$\delta(2\theta) = \frac{\lambda}{2\pi} \mathbf{k}_s \cdot \mathbf{r} - \frac{\lambda}{2\pi} \mathbf{k}_i \cdot \mathbf{r} = \frac{\lambda}{2\pi} (\mathbf{k}_s - \mathbf{k}_i) \cdot \mathbf{r} = \frac{\lambda}{2\pi} \mathbf{q} \cdot \mathbf{r}.$$

The corresponding phase difference is:

$$\varphi(2\theta) = \frac{2\pi}{\lambda} \delta(2\theta) = \mathbf{q} \cdot \mathbf{r}.$$

The amplitude of the scattered wave associated with the charge  $\rho(\mathbf{r})dV$  at position  $\mathbf{r}$  is  $A_s^{(e)} e^{i\varphi} \rho(\mathbf{r})dV$ . The expression  $e^{i\varphi} \rho(\mathbf{r})dV$  is called the *differential scattering amplitude*. For two small charges as described above, the total scattering amplitude is the sum of the amplitudes of the two scattered waves:

$$A_s(\mathbf{q}) = A_s^{(e)} e^{i\mathbf{q} \cdot \mathbf{0}} (\rho(\mathbf{0})dV) + A_s^{(e)} e^{i\mathbf{q} \cdot \mathbf{r}} (\rho(\mathbf{r})dV) = A_s^{(e)} (\rho(\mathbf{0}) + \rho(\mathbf{r}) e^{i\mathbf{q} \cdot \mathbf{r}}) dV.$$

Now, atoms have continuous, spherical distributions of electron density  $\rho(\mathbf{r})$  about the nucleus. Therefore, X-rays will be scattered by this distribution of electron density  $\rho(\mathbf{r})$  and the scattered waves will be the superposition of waves scattered by  $\rho(\mathbf{r})dV$  throughout the atom. Therefore, the *atomic scattering amplitude*  $A_s^{(Z)}(\mathbf{q})$  for an atom with atomic number  $Z$  is evaluated by integrating the differential scattering amplitude over the entire volume of the atom:

$$A_s^{(Z)}(\mathbf{q}) = \int A_s^{(e)} e^{i\mathbf{q} \cdot \mathbf{r}} \rho(\mathbf{r})dV = A_s^{(e)} \int e^{i\mathbf{q} \cdot \mathbf{r}} \rho(\mathbf{r})dV = A_s^{(e)} f_Z(\mathbf{q})$$

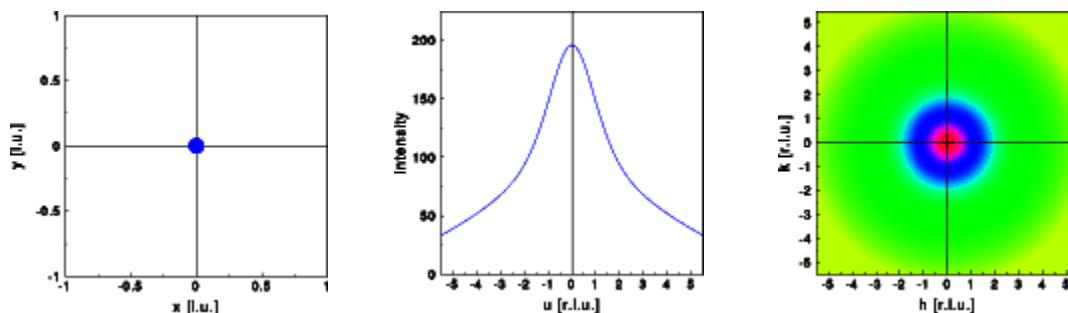
in which  $f_Z(\mathbf{q})$  is the *atomic scattering (form) factor* for the atom with atomic number  $Z$ .

**(9) Atomic Form Factors:** Since electron density in an atom or ion is spherically symmetric,  $\rho(\mathbf{r})$  depends only on the distance from the nucleus  $\rho(r)$  and the atomic form factor becomes

$$f_Z(q) = \int e^{i\mathbf{q}\cdot\mathbf{r}} \rho(\mathbf{r}) dV = 4\pi \int_0^\infty r^2 \rho(r) \frac{\sin qr}{qr} dr.$$

Therefore,  $f_Z(q \rightarrow 0) = Z$  and  $f_Z(q \rightarrow \infty) = 0$ . In other words, the atomic form factor for the scattered wave along the incident wavevector direction is the atomic number, and it approaches zero with increasing scattering angle. “Atomic” form factors can be evaluated for charged ions also. If an atom were a point, then there would be no interference effects and  $f_Z(q) = Z$  for all values of  $q$ . However, due to atomic or ionic sizes, which are comparable to the wavelength of X-rays, there is destructive interference that increases with scattering angle  $2\theta$ . The extent of this interference increases with the size of the atom or ion. For example,  $\text{Si}^{4+}$ ,  $\text{Na}^+$ , and  $\text{O}^{2-}$  each have 10 electrons, but the ions increase in size from  $\text{Si}^{4+}$  to  $\text{Na}^+$  to  $\text{O}^{2-}$ , which shows the most destructive interference. At large scattering angles, these atomic form factors become similar in magnitude.

Another interpretation of the atomic form factor  $f_Z(q)$  is as the *Fourier transform* of the electron density. In this picture, the units of the scattering vector  $\mathbf{q}$  are  $\text{length}^{-1}$  and these vectors belong to *reciprocal space*. If the electron density of an atom is described graphically as a small disk with finite size in *real space* (left) then the Fourier transform of this electron density can be represented by either a 1-dimensional or 2-dimensional plot. The 1-d plot (middle) shows how  $f_Z(q)$  varies as the length of the scattering vector increases. For the circular atom,  $f_Z(q)$  rapidly decreases and then asymptotically approaches 0 at large  $q$  values. In 2-d (right), a contour plot of the Fourier transform emphasizes that  $\mathbf{q}$  is a vector in reciprocal space. The contour plot shows circular (spherical) symmetry of the Fourier transform for this model circular atom.



The majority of X-ray scattering from an atom or ion occurs through interactions with tightly bound core electrons. Therefore, it is difficult to distinguish elements that have similar atomic numbers by X-ray diffraction alone unless the interatomic distances in a structure are critically examine. Furthermore, identifying and locating light (low  $Z$ ) atoms close to heavy (high  $Z$ ) atoms, e.g., H next to La, O next to Bi, is especially difficult, unless you can use diffraction data at large scattering angles where the relative atomic scattering factors from the two elements become closer. To ensure high quality diffraction data at large scattering angles means a high quality crystalline specimen. Another important aspect of atomic scattering by X-rays is if the incident X-ray wavelength is close to an absorption, which will excite a core electron into the continuum followed by essentially instantaneous relaxation back to the core state, then the atomic form factor develops *anomalous scattering* terms that are energy (wavelength/frequency) dependent:

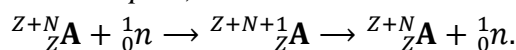
$$f_Z(q; \omega) = f_Z^0(q) + \Delta f'(\hbar\omega) + i\Delta f''(\hbar\omega).$$

The anomalous terms in the atomic form factor are independent of scattering vector but are dependent on the incident X-ray energy. Anomalous scattering affects the scattered intensities and can be useful for studying noncentrosymmetric structures. The effect has become increasingly useful with synchrotron radiation, which allows tunable X-ray wavelengths and large incident intensities.

The differential scattering cross section at the scattering angle  $2\theta$  for an atom  $Z$  is:

$$\frac{d\sigma}{d\Omega}(2\theta) = \left| A_s^{(Z)}(\mathbf{q}) \right|^2 = \left( r_0^2 P(2\theta) \right) |f_Z(\mathbf{q}; \omega)|^2.$$

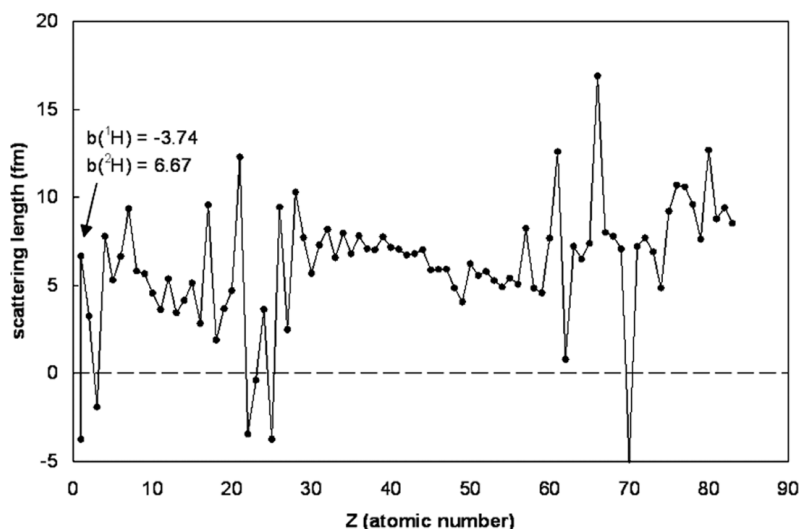
**(10) Atomic Scattering – Neutrons:** Since neutrons are electrically neutral, they are scattered by the nucleus and not by the much lighter electrons ( $m_{\text{neutron}} \approx 2000 m_{\text{electron}}$ ). Moreover, neutrons are spin- $1/2$  particles, so they may also be scattered by the presence of any unpaired electrons associated with atoms. For elastic scattering of neutrons, the scattering amplitude is a scattering “length”  $b$  (units of fm) that is independent of scattering angle  $2\theta$  and gives the scattering cross section  $\sigma = 4\pi b^2$ . During the scattering process, the neutron interacts with the nucleus to create an *activated complex*, which then scatters a neutron and leaves the original nucleus:



The activated complex is a short-lived isotope of the original nucleus. Given the existence of an activated complex, the nature of neutron scattering will vary from one isotope of an element to another. Many nuclei scatter neutrons *coherently* and elastically, but some nuclei scatter neutrons *incoherently*, which has two contributions: from spin incoherence (different atoms) and from isotopic incoherence (different isotopes). Spin incoherence arises from interactions of a neutron with nuclei with nonzero spin because the neutron spin could be either parallel or antiparallel to the nuclear spin during the scattering process. Isotopic incoherence arises from the distribution of different isotopes at any given atomic (nuclear) site that interacts with the neutron. Incoherent scattering is independent of scattering angle and contributes to the background of any diffraction pattern. In addition to incoherent scattering, absorption can be a concern, especially for certain isotopes of Gd, Sm, Cd, Dy, and B.

Each element/isotope is assigned coherent and incoherent scattering amplitudes  $b_{\text{coh}}$  and  $b_{\text{incoh}}$ . For example,  ${}^1\text{H}$  scatters neutrons incoherently ( $b_{\text{coh}} = -3.74$  fm;  $b_{\text{incoh}} = 25.18$  fm) whereas  ${}^2\text{H}$  ( ${}^2\text{D}$ ) scatters neutrons coherently ( $b_{\text{coh}} = +6.67$  fm;  $b_{\text{incoh}} = 3.99$  fm) and is very useful for locating hydrogen atoms. The presence of  ${}^1\text{H}$  in a sample creates large backgrounds over the entire observed scattering range and obscures many diffraction effects. The negative value of the coherent scattering amplitude for  ${}^1\text{H}$  means that there is a phase shift by  $\pi$  in the scattered wave from the incident wave. Below is a graph of coherent neutron scattering amplitudes (scattering lengths) vs. atomic number.<sup>2</sup> Atoms that scatter neutrons *incoherently* include  ${}^1\text{H}$  and isotopes of Sm, Gd, and Dy. Also, the scattering length for V is very small,  $b_{\text{coh}} \approx 0$  fm, which means that it hardly scatters neutrons at all. Therefore, vanadium is a useful container material for experiments.

<sup>2</sup> P.M.B. Piccoli, T.F. Koetzle, A.J. Schultz, *Comments Inorg. Chem.* **2007**, 28, 3-38.



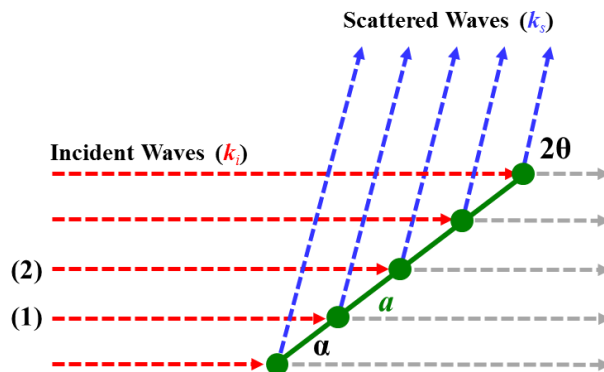
The variation in coherent scattering amplitudes with atomic number shows an overall slight increase along the periodic table. However, unlike scattering by X-radiation, it is generally easier to distinguish neighboring elements from each other as well as to locate light elements in the presence of heavy elements. The first effect arises from the significant fluctuations in neutron scattering by the activated complexes as a function of the number of nucleons; the second effect comes about because the differences in scattering lengths over the entire periodic table is much smaller than the corresponding scattering by X-rays.<sup>3</sup>

Since neutrons have intrinsic spin, they can also interact with magnetic moments caused by unpaired electrons and be scattered by these as well. Therefore, neutron diffraction can be used to extract both nuclear and magnetic ordering in crystalline samples.

**(11) X-ray vs. Neutron Scattering:** Neutron and X-ray diffraction are *complementary* techniques because X-ray diffraction gives the centers of electron density, whereas neutron diffraction gives the centers of nuclear density. Although both of these centers may coincide, they need not, especially if there is significant polarization of the electron density surrounding an atomic site by its environment. A combination of both techniques on the same sample can give detailed information of structure, electron density and interatomic forces within the solid-state structure that is inaccessible from a single technique.

**(12) von Laue Scattering:** Diffraction is useful for crystalline solids because of the conditions required for constructive interference of scattered radiation from a periodic array of atoms. The important results are the locations and intensities of diffraction spots, which are sites of constructive interference of superposition of scattered waves. Let's consider scattering from a 1-dimensional lattice of single atoms  $Z$  separated by distance  $a$ , and arbitrarily oriented at an angle  $\alpha$  with the direction of incident radiation, wavelength  $\lambda$ , has wavevector  $\mathbf{k}_i$ . Upon interacting with the atoms, we will observe scattered radiation along specific directions  $\mathbf{k}_s$  at scattering angles denoted as  $2\theta$ . This type of problem is called von Laue scattering, as depicted below.

<sup>3</sup> "Properties of the Neutron", J.K. Cockcroft, Birkbeck College, U. London (<http://pd.chem.ucl.ac.uk/pdnn/inst3/neutrons.htm>).



Coherent scattering between a pair of adjacent atoms in this chain gives rise to a phase difference  $\varphi(2\theta)$  in the scattered wave that is related to the path difference  $\delta(2\theta)$  traveled by the two rays:

$$\delta(2\theta) = a \cos \alpha - a \cos(2\theta - \alpha) = (\lambda/2\pi)(\mathbf{k}_s \cdot \mathbf{a} - \mathbf{k}_i \cdot \mathbf{a}) = (\lambda/2\pi)(\mathbf{k}_s - \mathbf{k}_i) \cdot \mathbf{a};$$

$$\varphi(2\theta) = 2\pi\delta(2\theta)/\lambda = (\mathbf{k}_s - \mathbf{k}_i) \cdot \mathbf{a} = \mathbf{q} \cdot \mathbf{a}.$$

$\mathbf{q}$  is the scattering vector with length  $q = 4\pi \sin \theta/\lambda$ . The scattering amplitude for scattering vector  $\mathbf{q}$  is the sum of all scattered wave amplitudes:

$$A_s(\mathbf{q}) = A_s^{(Z)}(\mathbf{q})[\dots + e^{iq(-a)} + e^{iq(0a)} + e^{iq \cdot a} + \dots]$$

$$= A_s^{(e)} \left[ f_Z(\mathbf{q}) \left( \sum_m e^{iq \cdot ma} \right) \right] = A_s^{(e)} \left[ f_Z(\mathbf{q}) \left( \frac{\sin(N\mathbf{q} \cdot \mathbf{a}/2)}{\sin(\mathbf{q} \cdot \mathbf{a}/2)} \right) \right].$$

The summation is taken over all  $N$  unit cells in the 1-dimensional crystal. Intensity rather than amplitude will be detected, so

$$I_s(\mathbf{q}) = |A_s(\mathbf{q})|^2 = r_0^2 P(2\theta) \left| f_Z(\mathbf{q}) \left( \sum_m e^{iq \cdot ma} \right) \right|^2 = r_0^2 P(2\theta) |f_Z(\mathbf{q})|^2 \frac{\sin^2(N\mathbf{q} \cdot \mathbf{a}/2)}{\sin^2(\mathbf{q} \cdot \mathbf{a}/2)}.$$

For constructive interference,  $\mathbf{q} \cdot \mathbf{a} = 2\pi(\text{integer})$ . Plotting the diffraction pattern as  $I_s(\mathbf{q})$  vs  $q$  gives peaks for the intensity at  $q = (2\pi/a)h$  for  $h = \text{integer}$ . As the number of unit cells  $N$  constituting the crystal increases, the diffraction peaks become sharper and the intensity between peaks falls to zero. The intensity expression also includes the variation of atomic form factor with scattering length. For X-rays, this function  $f_Z(\mathbf{q})$  decreases with increasing  $|h|$  and causes the diffraction intensity to decrease.

Since the scattering vectors  $\mathbf{q}$  for constructive interference are discrete, an important and useful construction that generalizes these vectors uses vector analysis. For this,  $\mathbf{a} = a\hat{\mathbf{a}}$ , which means that  $\mathbf{a}$  has length  $a$  in the direction of the unit vector  $\hat{\mathbf{a}}$ . Since  $\mathbf{q} \cdot \mathbf{a} = 2\pi h$ , the allowed scattering vectors  $\mathbf{q} = h(2\pi/a)\hat{\mathbf{a}}$ , i.e., the scattering vectors giving constructive interference for diffraction from a 1-d lattice have discrete lengths  $h(2\pi/a)$  and are directed parallel to the lattice vector  $\mathbf{a}$ . The vector  $h(2\pi/a)\hat{\mathbf{a}}$  is a *reciprocal lattice vector* because the length scale between lattice points is reciprocal distance, e.g.,  $\text{nm}^{-1}$  or  $\text{\AA}^{-1}$ . Because  $\mathbf{q}$  takes discrete values, it can be denoted as  $\mathbf{K}_h$ , i.e.,  $\mathbf{q} = \{\mathbf{K}_h; h = \text{integer}\}$  form a 1-dimensional *reciprocal space lattice* for the corresponding 1-dimensional *real space lattice*  $\{m\mathbf{a}; m = \text{integer}\}$ .

**(13)** In 3-dimensions, the crystal lattice involves three independent unit cell vectors and every lattice point is  $m\mathbf{a} + n\mathbf{b} + p\mathbf{c}$ ;  $m, n, p$  integers. The scattering amplitude for an allowed scattering vector  $\mathbf{q}$  is

$$A_s(\mathbf{q}) = A_s^{(e)} \left[ f_Z(\mathbf{q}) \left( \sum_{m,n,p} e^{i\mathbf{q}\cdot(m\mathbf{a}+n\mathbf{b}+p\mathbf{c})} \right) \right],$$

in which the summation is over all unit cells in the crystal. For constructive interference, then the allowed scattering vectors are restricted as follows:

$$\mathbf{q} \cdot (m\mathbf{a} + n\mathbf{b} + p\mathbf{c}) = 2\pi(\text{integer}).$$

As for the 1-d lattice, the vectors  $\mathbf{q}$  that satisfy this equation form a set of vectors of a 3-dimensional *reciprocal lattice* corresponding to the real space lattice. The unit cell of the *reciprocal lattice* is specified by vectors  $\mathbf{a}^*$ ,  $\mathbf{b}^*$ ,  $\mathbf{c}^*$  so that every scattering vector becomes:

$$\mathbf{q} = h\mathbf{a}^* + k\mathbf{b}^* + l\mathbf{c}^* = \mathbf{K}_{hkl}, \quad h, k, l = \text{integers, called } \textit{Miller indices}.$$

To construct the reciprocal lattice for any real space lattice, use the restriction

$$\mathbf{q} \cdot (m\mathbf{a} + n\mathbf{b} + p\mathbf{c}) = (h\mathbf{a}^* + k\mathbf{b}^* + l\mathbf{c}^*) \cdot (m\mathbf{a} + n\mathbf{b} + p\mathbf{c}) = 2\pi(\text{integer})$$

to set restrictions on  $\mathbf{a}^*$ ,  $\mathbf{b}^*$ ,  $\mathbf{c}^*$ :

$\mathbf{a}^*$  is perpendicular to  $\mathbf{b}$  and  $\mathbf{c}$  and its length is proportional to  $2\pi/a$ ;

$\mathbf{b}^*$  is perpendicular to  $\mathbf{a}$  and  $\mathbf{c}$  and its length is proportional to  $2\pi/b$ ;

$\mathbf{c}^*$  is perpendicular to  $\mathbf{a}$  and  $\mathbf{b}$  and its length is proportional to  $2\pi/c$ .

As a result of these restrictions, the following vector dot-product relationships hold:

$$\mathbf{a}^* \cdot \mathbf{a} = 2\pi \quad \mathbf{b}^* \cdot \mathbf{a} = 0 \quad \mathbf{c}^* \cdot \mathbf{a} = 0$$

$$\mathbf{a}^* \cdot \mathbf{b} = 0 \quad \mathbf{b}^* \cdot \mathbf{b} = 2\pi \quad \mathbf{c}^* \cdot \mathbf{b} = 0$$

$$\mathbf{a}^* \cdot \mathbf{c} = 0 \quad \mathbf{b}^* \cdot \mathbf{c} = 0 \quad \mathbf{c}^* \cdot \mathbf{c} = 2\pi.$$

These restrictions on the unit cell vectors of the reciprocal lattice ensure the phase conditions required for constructive interference:

$$(h\mathbf{a}^* + k\mathbf{b}^* + l\mathbf{c}^*) \cdot (m\mathbf{a} + n\mathbf{b} + p\mathbf{c}) = 2\pi(hm + kn + lp) = 2\pi(\text{integer}).$$

**(14) Reciprocal Lattice:** The diffraction peaks arising from constructive superposition of scattered waves from atoms forming a 3-d lattice occur at points described by the reciprocal lattice. The unit cell vectors  $\mathbf{a}^*$ ,  $\mathbf{b}^*$ ,  $\mathbf{c}^*$  of the reciprocal lattice are evaluated from the lattice vectors  $\mathbf{a}$ ,  $\mathbf{b}$ ,  $\mathbf{c}$  of the real space lattice of the crystal as follows:

Since  $\mathbf{a}^* \perp \mathbf{b}$  and  $\mathbf{c}$ , then  $\mathbf{a}^* = u(\mathbf{b} \times \mathbf{c})$ . Also,  $\mathbf{a} \cdot \mathbf{a}^* = \mathbf{a} \cdot u(\mathbf{b} \times \mathbf{c}) = uV = 2\pi$ , where  $V = \text{volume}$  of the unit cell formed by  $\mathbf{a}$ ,  $\mathbf{b}$ ,  $\mathbf{c}$ . Then,  $u = 2\pi/V$ . Using this algorithm to obtain  $\mathbf{b}^*$  and  $\mathbf{c}^*$ :

$$\mathbf{a}^* = \frac{2\pi}{V}(\mathbf{b} \times \mathbf{c}); \quad \mathbf{b}^* = \frac{2\pi}{V}(\mathbf{c} \times \mathbf{a}); \quad \mathbf{c}^* = \frac{2\pi}{V}(\mathbf{a} \times \mathbf{b}).$$

**PRIMITIVE MONOCLINIC LATTICE:** The unit cell vectors are  $\mathbf{a}$ ,  $\mathbf{b}$ ,  $\mathbf{c}$  with unrestricted angle  $\beta$  between  $\mathbf{a}$  and  $\mathbf{c}$  and angles  $\alpha = \gamma = 90^\circ$  so that  $\mathbf{b}$  is perpendicular to the  $\mathbf{ac}$ -plane. The reciprocal lattice vector  $\mathbf{a}^*$  is perpendicular to  $\mathbf{b}$  and  $\mathbf{c}$ . Since  $\mathbf{a}$  and  $\mathbf{c}$  are not orthogonal to each other,  $\mathbf{a}$  and  $\mathbf{a}^*$  are not parallel vectors; the angle between them is  $\beta - 90^\circ$ . Then

$$\mathbf{a} \cdot \mathbf{a}^* = (a)(a^*) \cos(\beta - 90^\circ) = (a)(a^*) \sin \beta = 2\pi$$

and the length of  $\mathbf{a}^*$  is  $2\pi/a \sin \beta$ . In the real space lattice,  $a \sin \beta$  is the distance between two adjacent  $\mathbf{bc}$ -planes. As a result, since  $\mathbf{a}^* = \mathbf{K}_{100}$ , then  $a \sin \beta = d_{100}$ , and the length of  $\mathbf{a}^*$  or  $\mathbf{K}_{100}$  is  $2\pi/d_{100}$ . Likewise,  $\mathbf{c}^* = 2\pi/c \sin \beta$ , so that  $\mathbf{c}^* = \mathbf{K}_{001}$  and  $d_{001} = c \sin \beta$ .

Therefore, in general, the reciprocal lattice vector  $\mathbf{K}_{hkl} = h\mathbf{a}^* + k\mathbf{b}^* + l\mathbf{c}^*$  is oriented perpendicular to planes of the real space lattice that are separated by a distance  $d_{hkl}$  and the length of  $\mathbf{K}_{hkl}$  is  $2\pi/d_{hkl}$ , i.e., inversely related to the separation between lattice planes.

**(15) Bragg's Law and Ewald Sphere:** As shown in slide (7), the scattering vector  $\mathbf{q} = \mathbf{k}_s - \mathbf{k}_i$  is the difference between the wavevectors for the scattered and incident waves. They are vectors  $\mathbf{K}_{hkl}$  of the reciprocal lattice with length  $2\pi/d_{hkl}$ . For elastic scattering, the lengths of  $\mathbf{k}_i$  and  $\mathbf{k}_s$  are  $2\pi/\lambda$ , so the three vectors  $\mathbf{q} = \mathbf{K}_{hkl}$ ,  $\mathbf{k}_i$ , and  $\mathbf{k}_s$  form an isosceles triangle with the angle between  $\mathbf{k}_i$  and  $\mathbf{k}_s$  being the scattering angle  $2\theta$ . From the interpretation of the reciprocal lattice,  $\mathbf{K}_{hkl}$  is perpendicular to lattice planes determined by the direction  $h\mathbf{a}^* + k\mathbf{b}^* + l\mathbf{c}^*$ . Two specific outcomes of this construction are:

- *Bragg's Law of Diffraction:* The isosceles triangle provides the following expression

$$\mathbf{k}_i \cdot \mathbf{K}_{hkl} = \frac{1}{2} |\mathbf{K}_{hkl}|.$$

If the wavevector  $\mathbf{k}_i$  starts on a reciprocal lattice point, then it ends on the plane bisecting  $\mathbf{K}_{hkl}$ . Since  $\mathbf{K}_{hkl}$  is perpendicular to lattice planes indexed as  $(hkl)$  in real space, these vectors define *Bragg planes*. Then,

$$\mathbf{k}_i \cdot \mathbf{K}_{hkl} = \left(\frac{2\pi}{\lambda}\right) \left(\frac{2\pi}{d_{hkl}}\right) \cos\left(\frac{\pi}{2} - \theta\right) = \left(\frac{2\pi}{\lambda}\right) \left(\frac{2\pi}{d_{hkl}}\right) \sin\theta = \frac{1}{2} \left(\frac{2\pi}{d_{hkl}}\right)^2 = \frac{1}{2} |\mathbf{K}_{hkl}|^2.$$

On rearranging, the Bragg equation results:  $\lambda = 2d_{hkl} \sin\theta$ .

- *The Ewald sphere:* If the incident wavelength for diffraction is a fixed value, then there are upper bounds placed on the integer values of  $h, k, l$  for the set of allowed scattering vectors  $\{\mathbf{q} = \mathbf{K}_{hkl}\}$ . Again, the isosceles triangle of  $\mathbf{K}_{hkl}$ ,  $\mathbf{k}_i$ , and  $\mathbf{k}_s$  gives the length of a scattering vector  $\mathbf{q} = \mathbf{K}_{hkl}$  to be  $4\pi \sin\theta/\lambda$ . Therefore,  $|\mathbf{K}_{hkl}| \leq 4\pi/\lambda$ , which sets the upper limits of observed diffraction indices for a diffraction experiment using fixed wavelength radiation. These limits in the values of  $h, k, l$  create the Ewald sphere. Another interpretation of this restriction is that observable diffraction occurs for the separation  $d_{hkl}$  between  $(hkl)$  Bragg planes to be at least  $\lambda/2$ .

**(16) Structure Factors:** Using the von Laue description of the scattering process, the total scattering amplitude from a 3-d lattice of a single type of atom  $Z$  is the superposition of the scattered waves from each atom:

$$A_{hkl} = A_{hkl}^{(e)} \sum_{m,n,p} f_Z(hkl) e^{2\pi i(hm+kn+lp)} = (-r_0 P^{1/2}(2\theta)) F_{hkl},$$

in which  $F_{hkl}$  is called the *structure factor*. The summation leads to constructive interference, i.e., nonzero values of  $F_{hkl}$ , only at the reciprocal lattice points  $\mathbf{K}_{hkl}$ . These positions, which are also labeled by the integer triple  $(hkl)$ , are called *reflections*. Although the summation is mathematically infinite, it is realistically a large sum. For an infinite sum, the structure factor will be delta functions at these reciprocal space points. However, because any crystal has *finite size*, the amplitudes will have some width. The broadening of diffraction peaks becomes significant if the domain size is less than about  $10^4$  unit translations.

Two important relationships for structure factors are: (i)  $F_{000} = NZ$ , where  $N = \#$  of unit cells included in the summation; and (ii)  $F_{\bar{h}\bar{k}\bar{l}} = F_{hkl}^*$ :

$$F_{000} = \sum_{m,n,p} f_Z(hkl) e^{2\pi i(0m+0n+0p)} = \sum_{m,n,p} f_Z(000) = \sum_{m,n,p} Z; \text{ and}$$

$$F_{\bar{h}\bar{k}\bar{l}} = \sum_{m,n,p} f_Z(hkl) e^{2\pi i(-hm-kn-lp)} = \sum_{m,n,p} f_Z(hkl) e^{-2\pi i(hm+kn+lp)} = F_{hkl}^*$$

In any diffraction experiment, only diffraction intensities and not scattering amplitudes are observed. Intensities are square amplitudes as follows:

$$I_{hkl} = |A_{hkl}|^2 \approx (r_0^2 P(2\theta)) |F_{hkl}|^2 = (r_0^2 P(2\theta)) F_{hkl} F_{hkl}^* = (r_0^2 P(2\theta)) F_{hkl} F_{\bar{h}\bar{k}\bar{l}} = I_{\bar{h}\bar{k}\bar{l}}$$

Therefore, diffraction patterns obey *Friedel's law*, which means that diffraction patterns have inversion symmetry. Although a crystal structure may be noncentrosymmetric, its diffraction pattern will be centrosymmetric, unless the crystal contains any anomalous scatterers for the incident radiation.

Most crystal structures have several atoms in the unit cell, so the next extension of the von Laue scattering problem is to consider scattering from a lattice with a *basis*, which is the collection of atoms within each unit cell. If the atoms are located at the sites with fractional coordinates  $(x_j, y_j, z_j)$  within one unit cell, then the structure factor  $F_{hkl}$  is the superposition

$$F_{hkl} = \sum_{m,n,p} \left( \sum_j f_j(hkl) e^{2\pi i(hx_j+ky_j+lz_j)} \right) e^{2\pi i(hm+kn+lp)} = \sum_{m,n,p} S_{hkl} e^{2\pi i(hm+kn+lp)}$$

Therefore, the structure factor is the summation of scattering over all atoms, but it is separated into summation within one unit cell before summation over the lattice. The term in parentheses is called the *geometrical structure factor*  $S_{hkl}$ . It represents adding up scattering amplitudes from the atoms within one unit cell. Therefore, interference effects by atoms within the unit cell, which are separated by distances smaller than distances within the lattice, can affect the observed intensities  $I_{hkl}$ .

**(17) Example (CsCl-Type Structure):** The space group is  $Pm\bar{3}m$  and the unit cell is  $a = b = c$  with  $\alpha = \beta = \gamma = 90^\circ$ . Atoms of type **A** occupy the site at  $(0,0,0)$ ; atoms of type **B** occupy the site  $(\frac{1}{2}, \frac{1}{2}, \frac{1}{2})$ . The geometrical structure factor is a sum over these two positions:

$$\begin{aligned} S_{hkl} &= f_A e^{2\pi i(0h+0k+0l)} + f_B e^{2\pi i(\frac{1}{2}h+\frac{1}{2}k+\frac{1}{2}l)} = f_A e^{i0} + f_B e^{i\pi(h+k+l)} \\ &= f_A + f_B (-1)^{h+k+l} = \begin{cases} f_A + f_B & h+k+l \text{ even} \\ f_A - f_B & h+k+l \text{ odd} \end{cases} \end{aligned}$$

Therefore, there is destructive interference coming from the unit cell contents for  $(hkl)$  reflections if  $h+k+l$  is an odd integer. For example,  $(hk0)$  reflections have large intensities for  $h+k =$  even integer, whereas  $(hk1)$  reflections have large intensities for  $h+k =$  odd integer.

If atoms **A** and **B** are the same, which creates the BCC structure, then reflections with odd integer  $h+k+l$  values will be completely absent, i.e., there will be no observed diffraction intensity:

$$S_{hkl} = f_A + f_A e^{i\pi(h+k+l)} = f_A (1 + (-1)^{h+k+l}) = \begin{cases} 2f_A & h+k+l \text{ even} \\ 0 & h+k+l \text{ odd} \end{cases}$$

Therefore, geometrical structure factors like  $S_{200}$ ,  $S_{011}$ ,  $S_{231}$  are  $2f_A$ , but those like  $S_{111}$ ,  $S_{021}$ ,  $S_{100}$  are 0. The effect for  $(hkl)$  reflections with odd  $h+k+l$  gives *systematic absences* in the diffraction pattern of a BCC crystal arising from the complete destructive interference between the atoms within the unit cell. Systematic absences occur for every centered lattice system and can help to assign lattice types and space groups from diffraction data.

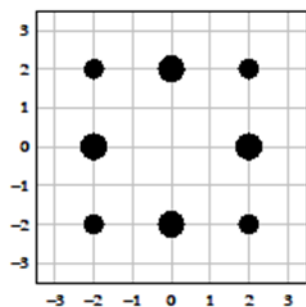
*Example 1 (FCC Structure):* The space group is  $Fm\bar{3}m$  and the unit cell is  $a = b = c$  with  $\alpha = \beta = \gamma = 90^\circ$ . Atoms of type **A** occupy the sites at  $(0,0,0)$ ,  $(\frac{1}{2}, \frac{1}{2}, 0)$ ,  $(0, \frac{1}{2}, \frac{1}{2})$ , and  $(\frac{1}{2}, 0, \frac{1}{2})$ . The geometrical structure factor is a sum over these four positions:

$$S_{hkl} = f_A e^{2\pi i(0h+0k+0l)} + f_A e^{2\pi i(\frac{1}{2}h+\frac{1}{2}k+0l)} + f_A e^{2\pi i(0h+\frac{1}{2}k+\frac{1}{2}l)} + f_A e^{2\pi i(\frac{1}{2}h+0k+\frac{1}{2}l)}$$

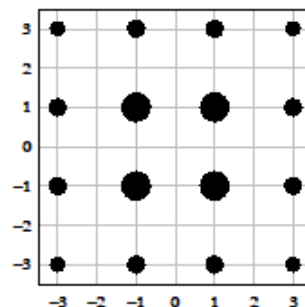
$$= f_A (1 + (-1)^{h+k} + (-1)^{k+l} + (-1)^{h+l}).$$

Since each Miller index  $h$ ,  $k$ , and  $l$  is either an even or an odd integer, there are 8 possible combinations ( $e$  = even;  $o$  = odd):  $(eee)$ ,  $(eeo)$ ,  $(eoe)$ ,  $(oeo)$ ,  $(ooe)$ ,  $(oee)$ ,  $(eoo)$ ,  $(ooo)$ . The only combinations that give nonzero values for  $S_{hkl}$  are  $(eee)$  and  $(ooo)$ . Therefore, the systematic absences for any face-centered lattice are identified by the reflection conditions for constructive interference: for any reflection  $(hkl)$ , the indices are either all even or all odd integers.

$(hk0)$  Plane:  
Since 0 is even,  
then  $h$  and  $k$  must  
also be even for  
constructive  
interference.



$(hk1)$  Plane:  
Since 1 is odd,  
then  $h$  and  $k$  must  
also be odd for  
constructive  
interference.



*Example 2 (Zinc Blende ZnS-Type Structure):* The space group is  $F\bar{4}3m$  and the unit cell is  $a = b = c$  with  $\alpha = \beta = \gamma = 90^\circ$ . Atoms of type **A** occupy the sites at  $(0,0,0)$ ,  $(\frac{1}{2}, \frac{1}{2}, 0)$ ,  $(0, \frac{1}{2}, \frac{1}{2})$ , and  $(\frac{1}{2}, 0, \frac{1}{2})$ ; atoms of type **B** occupy the sites at  $(\frac{1}{4}, \frac{1}{4}, \frac{1}{4})$ ,  $(\frac{3}{4}, \frac{3}{4}, \frac{1}{4})$ ,  $(\frac{1}{4}, \frac{3}{4}, \frac{3}{4})$ ,  $(\frac{3}{4}, \frac{1}{4}, \frac{3}{4})$ . The geometrical structure factor is a sum over these eight positions:

$$S_{hkl} = f_A e^{2\pi i(0h+0k+0l)} + f_A e^{2\pi i(\frac{1}{2}h+\frac{1}{2}k+0l)} + f_A e^{2\pi i(0h+\frac{1}{2}k+\frac{1}{2}l)} + f_A e^{2\pi i(\frac{1}{2}h+0k+\frac{1}{2}l)}$$

$$+ f_B e^{2\pi i(\frac{1}{4}h+\frac{1}{4}k+\frac{1}{4}l)} + f_B e^{2\pi i(\frac{3}{4}h+\frac{3}{4}k+\frac{1}{4}l)} + f_B e^{2\pi i(\frac{1}{4}h+\frac{3}{4}k+\frac{3}{4}l)} + f_B e^{2\pi i(\frac{3}{4}h+\frac{1}{4}k+\frac{3}{4}l)}.$$

This sum can be factored into

$$S_{hkl} = (f_A + f_B e^{2\pi i(\frac{1}{4}h+\frac{1}{4}k+\frac{1}{4}l)}) (1 + (-1)^{h+k} + (-1)^{k+l} + (-1)^{h+l})$$

$$= (f_A + f_B e^{i(\pi/2)(h+k+l)}) (1 + (-1)^{h+k} + (-1)^{k+l} + (-1)^{h+l}).$$

The first factor is from the 2 atoms of the *primitive unit cell*; the second factor is from the face-centered lattice. Therefore, the second factor sets the conditions for observing reflection  $(hkl)$  that the Miller indices are either all even or all odd. The first factor sets the following restrictions:

$$f_A + f_B e^{i(\pi/2)(h+k+l)} = f_A + f_B (i)^{h+k+l} = \begin{cases} f_A + f_B & h+k+l = 4n \\ f_A + if_B & h+k+l = 4n+1 \\ f_A - f_B & h+k+l = 4n+2 \\ f_A - if_B & h+k+l = 4n+3 \end{cases}$$

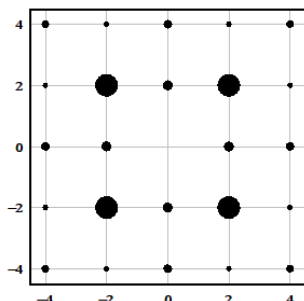
Therefore, for the ZnS-type structure, the only systematic absences are set by the face-centered lattice.

If atoms **A** and **B** are the same element, which gives the diamond-type structure, then this summation of the two sites of the primitive unit cell becomes:

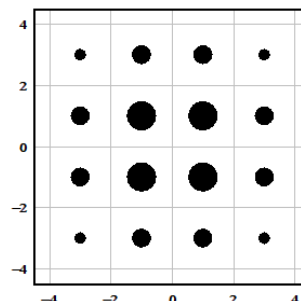
$$S_{hkl} = f_A (1 + (i)^{h+k+l}) = \begin{cases} 2f_A & h+k+l = 4n \\ f_A(1+i) & h+k+l = 4n+1 \\ 0 & h+k+l = 4n+2 \\ f_A(1-i) & h+k+l = 4n+3 \end{cases}$$

Thus, the diamond structure introduces additional systematic absences: if the indices of reflection ( $hkl$ ) are all even integers, then their sum  $h + k + l$  must be a multiple of 4.

( $hk0$ ) Plane:  
Since 0 is even,  
then  $h$  and  $k$  must  
also be even and  
 $h + k$  must be a  
multiple of 4 for  
constructive  
interference.



( $hk1$ ) Plane:  
Since 1 is odd,  
then  $h$  and  $k$  must  
also be odd  
without any other  
restrictions for  
constructive  
interference.



**(18) Determining Space Groups:** By measuring the scattering angles of diffraction peaks, the lattice parameters of the unit cell of a crystal can be determined. This is often an iterative process because knowledge of the ( $hkl$ ) indices for each reflection is necessary. Furthermore, the entire reflection pattern, which corresponds to the reciprocal lattice of the crystal, will have the rotational symmetry of one of the centrosymmetric crystallographic point groups, called *Laue classes*. This rotational symmetry of the diffraction pattern means that certain sets of reflections have equal intensities. Furthermore, we have already seen that centered lattices provide systematic absences in the diffraction pattern. In addition, the presence of screw rotations or glide reflections in the crystal structure will also introduce certain systematic absences. Therefore, identifying and understanding the rotational symmetry and systematic absences of a diffraction pattern are necessary to assign the space group of the crystal structure.

*Rotational Equivalences:* By Friedel's law for the intensities of scattering amplitudes,  $I_{\bar{h}\bar{k}\bar{l}} = I_{hkl}$ , diffraction patterns have inversion symmetry. When combined with the 7 crystal systems, this creates 11 Laue classes, which are the centrosymmetric crystallographic point groups. The following table summarizes the Laue classes and their corresponding point groups:

Crystal System	Laue Class	Point Groups			Equivalences (Generators)
Triclinic	$\bar{1}$	1	$\bar{1}$		$(\bar{h} \bar{k} \bar{l})$
Monoclinic ( $\parallel \mathbf{b}$ )	$2/m$	2	$m$	$2/m$	$(\bar{h} \bar{k} l)$ $(h k \bar{l})$
Orthorhombic	$mmm$	222	$mm2$	$mmm$	$(\bar{h} k l)$ $(h \bar{k} l)$ $(h k \bar{l})$
Tetragonal	$4/m$	4	$\bar{4}$	$4/m$	$(\bar{k} h l)$ $(h k \bar{l})$
	$4/mmm$	422	$4mm$	$\bar{4}2m$ $4/mmm$	$(\bar{k} h l)$ $(h k \bar{l})$ $(\bar{h} k l)$ $(k h l)$
Trigonal	$\bar{3}$	3	$\bar{3}$		$(\bar{k} h -k \bar{l})$ $(\bar{h} \bar{k} \bar{l})$
	$\bar{3}m$	32	$3m$	$\bar{3}m$	$(\bar{k} h -k \bar{l})$ $(h h -k l)$ $(\bar{h} \bar{k} \bar{l})$
Hexagonal	$6/m$	6	$\bar{6}$	$6/m$	$(h -k h l)$ $(h k \bar{l})$
	$6/mmm$	622	$6mm$	$\bar{6}m2$ $6/mmm$	$(h -k h l)$ $(h h -k l)$ $(h k \bar{l})$
Cubic	$m\bar{3}$	23	$m\bar{3}$		$(\bar{h} k l)$ $(k l h)$ $(\bar{h} \bar{k} \bar{l})$
	$m\bar{3}m$	432	$\bar{4}3m$	$m\bar{3}m$	$(\bar{h} k l)$ $(k l h)$ $(k h l)$ $(\bar{h} \bar{k} \bar{l})$

The last column identifies reflections equivalent to the general ( $hkl$ ) reflection, listed as *generators*. To see how these work, we'll examine the tetragonal system:

Laue class  $4/m$  has the two generators:  $4_c = 4$ -fold rotation with respect to  $c$ -axis and  $m_c =$  mirror perpendicular to  $c$ -axis. For a general reflection  $(hkl)$ , i.e., no restrictions on the integer values of  $h$ ,  $k$ , and  $l$ , the 4-fold rotation generates the equivalent reflections:  $(\bar{k}hl)$ ,  $(\bar{h}\bar{k}l)$ , and  $(k\bar{h}l)$ . For each of these reflections, the horizontal mirror generates:  $(hk\bar{l})$ ,  $(\bar{k}h\bar{l})$ ,  $(\bar{h}\bar{k}\bar{l})$ , and  $(k\bar{h}\bar{l})$ . Therefore, there are 8 rotationally equivalent  $(hkl)$  reflections in this Laue class; the number equals the order of the centrosymmetric point group. If certain subsets of reflections are examined, such as  $(hk0)$ , then the equivalence condition is  $(hk0) = (\bar{k}h0) = (\bar{h}\bar{k}0) = (k\bar{h}0)$ . In another terminology, the *multiplicity* of  $(hk0)$  reflections in this Laue class is 4. The only rotational symmetry observable for this plane of diffraction reflections is  $\mathcal{C}_4$ .

Laue class  $4/mmm$  has additional reflection symmetry operations. Therefore, the general reflection  $(hkl)$  has 16 rotationally equivalent reflections. This equivalent condition generates a multiplicity of 8 for  $(hk0) = (hk0) = (hk0) = (hk0) = (hk0) = (hk0) = (hk0) = (hk0)$ . Therefore, the diffraction pattern of the  $(hk0)$  plane exhibits two sets of mirror planes and 4-fold rotational symmetry.

**Systematic Absences:** While rotations and mirrors create equivalencies, centered lattices, screw rotations, and glide reflections create systematic absences in diffraction patterns. These systematic absences do not affect the rotational symmetry of a diffraction pattern, but they help to assign space groups. Systematic absences are reciprocal lattice points where there is zero diffraction intensity. They arise from destructive interference accomplished by certain spatial relationships between atoms in a unit cell. Therefore, these absences arise within the geometrical structure factors. The following table summarizes some systematic absences:

Lattice Centering	Reflection Condition	Screw Axes	Reflection Condition	Glide Planes	Reflection Condition
$I$	$h + k + l$ even	$2_1, 4_2, 6_3 \parallel c$	$(00l), l$ even	$a \perp c$	$(hk0), h$ even
$F$	$h, k, l$ all even or all odd	$3_1, 3_2, 6_2, 6_4 \parallel c$	$(00l), l = 3N$	$b \perp c$	$(hk0), k$ even
$C$	$h + k$ even	$4_1, 4_3 \parallel c$	$(00l), l = 4N$	$n \perp c$	$(hk0), h + k$ even

**(19) Phase Problem:** In the diffraction experiment, intensities of the scattered radiation are measured rather than scattering amplitudes. Intensities are proportional to the square of the scattering amplitudes, i.e.,  $I_{hkl} \propto |F_{hkl}|^2$ . According to Friedel's law, the observed diffraction pattern will have inversion symmetry, i.e.,  $I_{\bar{h}\bar{k}\bar{l}} = I_{hkl}$ , even though the structure itself may not have inversion symmetry. This result arises because the structure factor  $F_{hkl}$  is a complex number and  $F_{\bar{h}\bar{k}\bar{l}} = (F_{hkl})^*$ . Now, the *goal* of the X-ray diffraction experiment is to determine the electron density, which is the inverse Fourier transform of the structure factors, from the measured intensities and their positions:

$$\rho(\mathbf{r}) = \frac{1}{V} \sum_{h,k,l} F_{hkl} e^{-i\mathbf{K}_{hkl} \cdot \mathbf{r}} = \frac{1}{V} \sum_{h,k,l} |F_{hkl}| e^{i\varphi_{hkl}} e^{-i\mathbf{K}_{hkl} \cdot \mathbf{r}}.$$

Every structure factor  $F_{hkl} = |F_{hkl}| e^{i\varphi_{hkl}}$  is a complex number, but all that is obtained from the diffraction experiment is its amplitude  $|F_{hkl}|$ . This issue is called the *phase problem*, which creates the challenges for solving diffraction problems. If both scattering amplitudes and phases could be measured, then the inverse Fourier transform to obtain the electron density would be a straightforward computational exercise.

A simple demonstration of the phase problem is seen by considering two atoms  $Z$  at the different positions  $x = 0$  and  $x = 0.5a$ . The scattering amplitude for the scattering vector  $q$  is  $F(q) = f_Z(q)e^{2\pi i q x}$ . For the atom at  $x = 0$ ,  $F(q) = f_Z(q)$  and  $I(q) = |F(q)|^2 = f_Z^2(q)$ . For the atom at  $x = 0.5a$ ,  $F(q) = f_Z(q)e^{i\pi q} = f_Z(q) \cos q\pi + i f_Z(q) \sin q\pi$ . This wave has both real and imaginary components. However,  $I(q) = |F(q)|^2 = F^*(q)F(q) = f_Z^2(q)$ , which is identical to the intensity of scattering from the atom at  $x = 0$ . Therefore, scattered intensities are insensitive to where the origin of the coordinate system is placed. However, without knowing the phase of the scattered wave, complete information about an atom's position relative to a specific origin cannot be clearly solved.

**(20)** There are some important strategies used to overcome the phase problem during the solution steps of X-ray diffraction experiments:

- (a) *Direct Methods*: This strategy is a statistical analysis of the data, and derives structure factor phases from the observed amplitudes using mathematical techniques based upon two important properties of the electron density: (i)  $\rho(\mathbf{r}) \geq 0$ , it is everywhere positive; and (ii)  $\rho(\mathbf{r})$  includes the positions of discrete atoms, so that data are measured to atomic resolution with minimum  $d$ -spacings of 0.9-1.0 Å. As a statistical method, it is important that the number of structure amplitudes measured be sufficiently larger, i.e., by a factor of  $\sim 10$ , than the number of structural parameters (atomic coordinates) to be determined. Direct methods works best if the atoms are uniformly distributed throughout the unit cell and have relatively similar scattering powers. Relationships between amplitudes that can lead to determination of phases involve Harker-Kasper inequalities and Sayre's relationships among the signs of  $F_{hkl}$ 's. In software packages used for structure solution from single crystal X-ray diffraction data, this approach is often the default.
- (b) *Patterson Function (Heavy-Atom) Method*: The Patterson function  $P(\mathbf{u})$  in real space is an example of a *vector method* to determine phases and is obtained directly from the observed intensities ( $I_{hkl} \propto |F_{hkl}|^2$ ):

$$P(\mathbf{u}) = \frac{1}{V^2} \sum_{h,k,l} |F_{hkl}|^2 e^{iK_{hkl} \cdot \mathbf{u}}; \quad \mathbf{u} = \mathbf{r}_j - \mathbf{r}_i$$

$P(\mathbf{u})$  gives peaks at positions  $\mathbf{u}$  that represent vectors between pairs of atoms  $\mathbf{r}_j - \mathbf{r}_i$ . The peak intensity is proportional to  $Z_i Z_j$ , i.e., the product of atomic numbers for the two atoms of the pair. This peak is quite intense if the vector connects two heavy, high- $Z$  elements. Once these heavy elements are successfully located, then phases can be evaluated using these atoms and their positions. These phases then are used to locate the lighter atoms in the structure.

Once a model structure has been proposed, then the atomic parameters must be refined to establish the best possible correspondence between the observed structure factor amplitudes and the ones obtained from the model. A common method of assessing this agreement is to calculate residual (reliability) indices. Two examples are

$$R_1 = \frac{\sum ||F_{hkl}(\text{obs})| - |F_{hkl}(\text{calc})||}{\sum ||F_{hkl}(\text{obs})||} \quad \text{and} \quad wR_2 = \left[ \frac{\sum w (F_{hkl}^2(\text{obs}) - F_{hkl}^2(\text{cal}))^2}{\sum w F_{hkl}^2(\text{obs})} \right]^{1/2}.$$

The summations are over all observed scattering events (reflections) and  $w = 1/\sigma^2(F_{hkl}(\text{obs}))$  with  $\sigma(F_{hkl}(\text{obs})) =$  standard deviation of  $F_{hkl}(\text{obs})$ .

**(21) Anomalous Scattering:** If an atom has an absorption edge just above the wavelength of the incident X-rays, then that atom can scatter X-rays *anomalously*, arising from a phase delay of the scattered radiation. In general, an atom  $Z$  in a sample will interact with an incident X-ray photon in one of the following ways:

- Normal scattering of an X-ray: the incident X-ray will typically have an energy low with respect to any transition in the atom. The atomic scattering factor is just  $f_Z^{(0)}$ .
- Fluorescence: the incident X-ray is absorbed by the atom, which re-emits an X-ray photon at lower energy. Fluorescence creates significant background, which can obscure weak Bragg reflections in a diffraction pattern, as occurs for Fe samples using Cu  $K\alpha$ -radiation.<sup>4</sup>
- Anomalous scattering: the incident X-ray is absorbed and re-emitted at the same energy, but the scattered wave has a phase change. The resulting atomic scattering factor includes a frequency-dependent term,  $f_Z = f_Z^{(0)} + f_Z^{(AS)}(\omega) = f_Z^{(0)} + f_Z'(\omega) + if_Z''(\omega)$ , which includes the phase change.

Anomalous scattering of X-rays can be used advantageously to study *noncentrosymmetric* structures, i.e., those structures that do not have inversion symmetry. An important early demonstration of this effect was reported in 1930 by examining the ratios of diffracted (111) vs. ( $\bar{1}\bar{1}\bar{1}$ ) intensities from cubic ZnS using Au  $L\alpha_1$  and Au  $L\alpha_2$  incident radiation. The  $K$  absorption edge for Zn falls just below the energy of the Au  $L\alpha_1$  energy and shows an “anomalous” effect to its scattering factor. Given the lack of inversion of the zinc blende structure, different scattered intensities were observed.<sup>5</sup>

**(22)** To see how anomalous scattering works breaks Friedel’s law, consider a 1-d chain consisting of two atoms in the unit cell: **A** at  $x = 0$  and **B** at  $x = x_B a$ . The structure factors and corresponding intensities are:

$$F_h = \sum_m (f_A + f_B e^{2\pi i h x_B}) e^{2\pi i h m} = \sum_m S_h e^{2\pi i h m};$$

$$I_h = |F_h|^2 = \sum_{m,m'} S_h^* S_h e^{2\pi i h(m-m')} = \sum_{m,m'} |S_h|^2 e^{2\pi i h(m-m')} = |S_h|^2 \sum_{m,m'} e^{2\pi i h(m-m')} \propto |S_h|^2.$$

The summation is over all unit cells in the 1-d crystal and gives rise to the Bragg diffraction peaks for all integers  $h$  from the constructive interference throughout the crystal. Any anomalous scattering effects occur in the geometrical structure factor, so that we can focus on this term. A centrosymmetric structure has  $x_B = 0.5$ ; an example of a noncentrosymmetric structure has  $x_B = 0.6$ . Then, consider the following two scenarios:

- (I) **A** = normal scatterer,  $f_A = f_A'$ ;  
**B** = normal scatterer,  $f_B = f_B'$ .

With these atomic scattering factors, evaluate the geometrical structure factors for the centrosymmetric and noncentrosymmetric structures:

$$S_h(\text{centro}) = f_A' + f_B' e^{i\pi h} \quad I_h \propto |S_h|^2 = f_A'^2 + f_B'^2 + 2f_A'f_B' \cos \pi h$$

Therefore,  $|S_h|^2 = |S_h|^2$ ; Friedel’s law obeyed.

$$S_h(\text{noncentro}) = f_A' + f_B' e^{1.2\pi h i} \quad I_h \propto |S_h|^2 = f_A'^2 + f_B'^2 + 2f_A'f_B' \cos 1.2\pi h$$

<sup>4</sup> Y.M. Mos, A.C. Vermeulen, C.J.N. Buisman, J. Weijma, *Geomicrobiol. J.* **2018**, 35, 511-517.

<sup>5</sup> W. A. Hendrickson, *Q. Rev. Biophys.*, **2014**, 47, 49-93.

Therefore,  $|S_{\bar{h}}|^2 = |S_h|^2$ ; Friedel's law obeyed.

For both structures, the X-ray diffraction pattern follows Friedel's law.

(II) **A** = anomalous scatterer,  $f_A = f'_A + if''_A = f'_A + f''_A e^{i\pi/2}$

**B** = normal scatterer,  $f_B = f'_B$ .

Again, evaluate the geometrical structure factors for the centrosymmetric and noncentrosymmetric structures:

$$S_h(\text{centro}) = f'_A + f''_A e^{i\pi/2} + f'_B e^{i\pi h}$$

$$I_h \propto |S_h|^2 = f_A'^2 + f_A''^2 + f_B'^2 + 2f'_A f'_B \cos \pi h$$

Therefore,  $|S_{\bar{h}}|^2 = |S_h|^2$ ; Friedel's law obeyed.

$$S_h(\text{noncentro}) = f'_A + f''_A e^{i\pi/2} + f'_B e^{1.2\pi h i}$$

$$I_h \propto |S_h|^2 = f_A'^2 + f_A''^2 + f_B'^2 + 2f'_A f'_B \cos 1.2\pi h + 2f''_A f'_B \sin 1.2\pi h$$

Therefore,  $|S_{\bar{h}}|^2 \neq |S_h|^2$ ; Friedel's law is not obeyed.

In general, the effect is small. Nonetheless, such differences in the intensities of reflections related by inversion can help immensely to solve noncentrosymmetric structures. This effect was used by Jerome and Isabelle Karle to solve the structures of protein molecules using X-ray diffraction.<sup>6</sup>

**(23) Factors affecting Intensities:** Numerous factors affect the intensities of scattered X-rays. We have already seen that the interference effects of X-ray scattering by the electron densities of atoms will cause intensities to decrease as the scattering angle increases. Other factors arise, and these can be separated into *geometrical* and *physical* factors.<sup>7</sup> Geometrical factors depend upon how the diffraction experiment is set up, i.e., the instrumentation; physical factors depend upon the sample and how the atoms in the sample interact with and scatter radiation. They include:

- The *Lorentz factor*, which describes how a reciprocal lattice point, which specifies the location of scattering of constructive interference, passes through the reflection condition. In the X-ray diffraction experiment for a single crystal, the crystal lattice has an arbitrary orientation with respect to the incident X-ray beam. Therefore, the crystal must be moved, i.e., rotated, to obtain a positive reflection condition. Since diffraction peaks have widths due to the finite size of the lattice domains, and since these widths need not be *isotropic*, i.e., the same size in all directions, then, as the diffraction peak moves through the detector, it can move through at different speeds, which depends on the scattering angle. The Lorentz factor is defined by  $L(2\theta) = \omega/\lambda v_n$ , with  $\omega$  = angular velocity of crystal rotation on the diffractometer,  $\lambda$  = incident X-ray wavelength, and  $v_n$  = velocity component of the Bragg reflection perpendicular to the Ewald sphere surface, which is the condition for an observable diffraction peak. Typically,  $L(2\theta)$  varies as  $1/\sin 2\theta$  (for powder diffraction,  $L(2\theta) \sim 2/\sin \theta \sin 2\theta$ ).
- The *polarization factor* is always present for X-rays, which are scattered by electrons. This factor depends on the scattering angle according to  $(1 + \cos^2 2\theta)/2$ , which was shown for X-ray scattering by a single free electron. If X-rays are diffracted by a monochromator, then the polarization is also affected by scattering of the monochromator, with angle  $2\theta_M$ . The Lorentz and polarization factors are typically combined into a single term.

<sup>6</sup> <http://skuld.bmsc.washington.edu/scatter/>, Ethan A. Merritt at U. Washington.

<sup>7</sup> B.E. Warren *X-Ray Diffraction*, Addison-Wesley, Reading, MA, 1969.

- A *multiplicity factor*, which is important for powder diffraction rather than single crystal diffraction, arises from any rotational symmetry possessed by the crystalline structure. When a crystal has twofold, threefold, fourfold, or sixfold symmetry, some reflections labeled by the Miller indices ( $hkl$ ) will be related to each other. Then, diffraction with these related scattering vectors will build up at the same scattering angle. Furthermore, different ( $hkl$ ) scattering vectors, which are unrelated by rotational symmetry, can also yield identical scattering angles and affect the observed intensities, if the geometrical structure of the unit cell is appropriate. (See discussion on powder diffraction below).

Physical factors include:

- *Absorption* always occurs and follows Beer's law,  $I = I_0 e^{-\mu d}$ , in which  $d$  = distance that X-radiation travels through the sample. It is best for a crystalline sample to have a spherical shape, then absorption is the same in all directions and will not affect relative intensities. However, if the crystalline shape is anisotropic, then intensities will be affected by how the crystal is oriented relative to the incident X-ray beam. Absorption coefficients tend to increase with atomic number, so samples of heavy elements should be as small as possible to decrease absorption issues, which will have the greatest impact on the observation of high-angle reflections.
- *Extinction* occurs if a crystal is "too perfect," i.e. if the lattice planes are perfectly parallel with each other. If an incident wave satisfies the Bragg condition, then its scattered wave will have an angle  $2\theta$  with respect to the incident wave and an angle  $\theta$  with respect to the lattice planes giving rise to the reflection. However, the scattered wave from any interior plane will satisfy the Bragg reflection condition for other lattice planes as it emerges from the specimen and undergoes *secondary reflection*; this secondary reflection travels parallel with the primary (incident) beam. Since the scattered radiation expresses a phase change by  $\pi/2$ , two successive Bragg reflections lead to a net phase change of  $\pi$  and the secondary beam will be completely out-of-phase with the primary beam and attenuate the overall primary beam. Such attenuations can occur for other reflected beams due to the crystal perfection and become significant if crystal perfection covers a large crystalline volume. Thus, crystalline samples that are optimal for diffraction experiments are said to express good *mosaic character*, which generally occurs naturally via structural and lattice defects. However, many crystals that are grown under high pressure over long time periods (geological samples, for example) can show high degrees of "perfection" and exhibit significant extinction effects
- Fluctuations of atomic positions (*displacements*) due to temperature affect intensities. As the temperature of a sample increases, the electrons "sweep out" a larger average volume. This effective size change of the atoms affects the atomic scattering factors:  $f_Z(q)$  falls off more rapidly with  $q$  than that for a rigid atom. This effect is modeled by a Debye-Waller factor:

$$f_Z = f_Z^{(0)} e^{-B \sin^2 \theta / \lambda^2}.$$

The Debye-Waller factor is  $B = 8\pi^2 \langle u^2 \rangle$ , where  $\langle u^2 \rangle$  is the root-mean-square displacement of the electron density associated with the atom. Accordingly,  $B$  has units of squared length.

**(24)** Detecting scattered (diffracted) X-radiation involves using either serial or parallel methods. The intensity of scattered radiation is, in general,

$$I_{hkl} \sim k \cdot A(V, \lambda, 2\theta) \cdot LP(2\theta) \cdot |F_{hkl}|^2,$$

which contains absorption, Lorentz-polarization, and structure factor terms. Serial methods are seldom used in modern diffraction instrumentation because it lacks the speed offered by parallel

methods. In a serial detection method, diffraction events are collected one at a time; in a parallel detection method, several scattering events are collected simultaneously. The primary serial method uses a scintillation detector, e.g., a NaI scintillation crystal. In this detector, X-rays pass through a Be window to the scintillator, which transmits through a phototube to convert light into current, which is amplified and analyzed. A scintillation detector shows very good angular resolution, is fast for a single detection event, and is inexpensive, but records just a single scattering event at a time. The detector must be moved to meet the diffraction conditions. Therefore, collecting data by serial means is quite time consuming.

Parallel methods include (a) film, which is inexpensive and quick, but there is poor angular and energy resolution; (b) position-sensitive detectors and image plates; (c) charge-coupled device (CCD) arrays; and (d) hybrid photon counters. For image plates, an imaging phosphor produces a latent image formed by X-ray exposure that is subsequently read by laser-stimulated luminescence. Important phosphors include  $\text{Gd}_2\text{O}_2\text{S:Tb}$ ,  $\text{Gd}_2\text{O}_2\text{S:Eu}$ , and  $\text{CdWO}_4$ . The phosphor is erased and re-used. Hybrid photon counters utilized semiconductor sensors and readout electronics.<sup>8</sup>

**(25)** Powder diffraction is a standard method of structural and chemical analysis in solid-state chemistry. It is a 1-dimensional measurement of diffraction intensity vs. scattering angle and requires a polycrystalline mixture of randomly oriented crystalline grains. Since a diffraction pattern is intrinsically 3-dimensional, some information is lost by powder diffraction. Therefore, it is difficult to *solve* unknown structures using powder diffraction data alone, but it is exceedingly effective to identify phases using expected patterns based upon known crystal structure data. On the other hand, *single crystal diffraction* is an important complementary characterization tool because crystal structures can be effectively solved and refined from the intrinsic 3-d data that are collected. A combination of single crystal and powder diffraction information can provide very accurate interatomic distances and thermal displacement parameters about equilibrium positions: atomic positions and thermal parameters are obtained from single crystal results; accurate lattice constants are obtained from powder results.

The diffraction intensities observed from a single crystal are single points, which are characterized by their location given by a vector of the reciprocal lattice  $\mathbf{K}_{hkl}$ . Their positions lie on the circular bases of cones whose axis is the direction of the incident radiation, and the angles of the cones are the allowed scattering angles  $2\theta$ . Due to crystallite sizes and intrinsic fluctuations in electron densities throughout a crystal, each diffraction “point” is a peak, broadened by these effects. Detection of diffraction intensities involves moving the crystalline specimen into an orientation to satisfy the geometry of the detector, whether it is a serial or parallel detector. Many single crystal diffractometers use monochromatic X-radiation with the crystal mounted in a Eulerian cradle, which allows variation of four “circles:  $2\theta$  (the scattering angles for diffraction;  $\omega$  (coaxial with  $2\theta$ );  $\chi$  (rotation in plane perpendicular to the  $2\theta/\omega$  axis); and  $\varphi$  (axis perpendicular to  $\chi$  but with variable orientation relative to the  $2\theta/\omega$  axis). Such a *four-circle diffractometer* allows access to all reciprocal lattice positions that satisfy the Ewald sphere condition ( $|\mathbf{K}_{hkl}| \leq 4\pi/\lambda$ ), barring any mechanical collisions between the circle mechanism and detector as well as possible shadowing effects).

**(26)** Diffraction intensities from an *ideal powder* sample will be the result of diffraction from a quasi-infinite number of distinct grains or crystallites that are randomly oriented, so that the diffraction condition creates rings that form the bases of each scattering cone. Each crystalline grain  $n$  gives a diffraction pattern,  $I_{hkl}(n) \propto |F_{hkl}(n)|^2$ , in which  $n$  labels the grain, and the pattern

<sup>8</sup> A. Förster, S. Brandstetter, C. Schulze-Briese, *Phil. Trans. R. Soc. A* **2019**, A377, 20180241.

is oriented as the crystal lattice is oriented. If there are several, randomly oriented grains, then there will be a superposition of the individual diffraction patterns, i.e., a superposition of *intensities*, not scattering amplitudes, because there are no interference effects between grains. Therefore,  $I_{hkl} = \sum_n I_{hkl}(n)$ , which is not the same expression as  $(\sum_n |F_{hkl}(n)|)^2$ . As the number of grains in the sample increases, the diffraction pattern becomes circular rings. The diffractometer samples just *one direction away from the origin*.

An important assumption for a proper powder diffraction pattern is that there are several, randomly oriented grains. If there are just a few grains, the powder diffraction experiment will not sample reciprocal space homogeneously, so some peaks will show much lower intensities than expected. Along this line of reasoning, if certain crystallographic planes of the microscopic structure are not randomly oriented, even if there are a sufficient number of grains, then the relative intensities of observed reflections will not match expectations from the structure for a completely random set of grains. The pattern is said to display preferred orientation, which can be common for layered structures like MoS<sub>2</sub>.

**(27)** According to the Bragg equation,  $\lambda = 2d_{hkl} \sin \theta_{hkl}$ , there are two experimental variables to use for detecting diffraction intensities from a given crystal, which will contain specific lattice plane spacings  $d_{hkl}$ . These variables are either the wavelength of incident radiation or the scattering angles.

Using *film* or any type of *parallel-mode* detection, a continuous loop of the detector is constructed to collect as much scattering as possible for a fixed incident wavelength  $\lambda$ . The film intersects the diffraction cones and is sufficiently narrow to produce distinct lines on the film, observations that are measured relative to the incident beam. This approach is called the *Debye-Scherrer* technique. Special focusing of the X-ray beams are characteristic of Guinier cameras, which give superb angular resolution and very accurate lattice constants ( $\pm 0.0005 \text{ \AA}$ ). On the other hand, *time-of-flight* detection involves placing detectors at specific angles. In this case, the scattering angles  $2\theta$  are fixed, and the continuous kinetic energies of neutrons create the diffraction pattern because  $\lambda$  varies. Synchrotron radiation also can involve variable wavelength X-rays using fixed angle detector banks.

An alternative construction for X-ray powder diffractometers is the *Bragg-Brentano* geometry in which the polycrystalline sample is oriented at angle  $\omega = \theta$  with respect to the incident X-ray beam and the scattering vectors for diffraction are always perpendicular to the surface of the sample. In a  $\theta:2\theta$  instrument, the X-ray source tube is fixed, the sample is rotated at  $\theta/\text{min}$  while the detector is rotated at  $2\theta/\text{min}$ . In a  $\theta:\theta$  instrument, the sample is fixed, the X-ray source tube rotates at  $-\theta/\text{min}$  and the detector rotates at  $+\theta/\text{min}$ .

**(28)** Powder diffraction is used for *fingerprinting*, i.e., phase identification, as well as to obtain very accurate lattice constants for determination of accurate interatomic distances. As long as there are no physical effects influencing the diffraction pattern, a determination of yields using relative intensities can provide semi-quantitative analysis, providing all products in the sample are crystalline. This fingerprinting ability allows powder diffraction to be widely used to establish phase diagrams, in concert with thermal analysis.

A significant advancement for solving crystal structures using neutron diffraction patterns was the discovery and development of the *Rietveld refinement* method,<sup>9</sup> which is an algorithm to match the complete diffraction pattern over the entire collection range, i.e., to match all regions of both

---

<sup>9</sup> H.M. Rietveld, *J. Appl. Cryst.* **1969**, 2, 65-71.

constructive and destructive interference. There are two aspects to a successful Rietveld refinement: (1) fitting peak profiles, i.e., peak shapes, as a function of scattering angle; and (2) fitting peak intensities, which are the integrated areas associated with each peak. Profile fitting is a numerical procedure that relates peak shape with scattering angle. The Rietveld method was originally developed to analyze neutron diffraction patterns because the scattering factors from atoms (nuclei) are isotropic and independent of scattering angle. Diffraction peaks follow a Gaussian shape. Applying Rietveld methods to X-ray diffraction patterns took many years of numerical and statistical development because atomic scattering factors depend on scattering angle in a complicated manner. Current peak shapes in X-ray diffraction patterns are fit using a combination of Lorentzian and Gaussian functions, which are called pseudo-Voigt functions. The peak intensities are related to the distribution of electron or nuclear density within the unit cell. Thus, accurate fitting of the peak areas gives a sound structural model. Therefore, to obtain accurate areas, the peak shapes must be well understood, so a complete Rietveld analysis involves an iterative process between fitting peak profiles and peak areas.

**(29)** In a powder diffraction pattern, every peak is characterized by its position and its width. According to the Bragg equation,  $\lambda = 2d_{hkl} \sin \theta_{hkl}$ , the peak positions are one-half the scattering angles  $2\theta_{hkl}$  and give information about the various distances between Bragg planes in real space,  $d_{hkl}$ , which are called  $d$ -spacings. The expressions of  $1/d_{hkl}^2$  for the various crystal classes are summarized:

Crystal System	Unit Cell Parameters	$\frac{1}{d_{hkl}^2} = \frac{4 \sin^2 \theta_{hkl}}{\lambda^2}$
Cubic	$a = b = c$ $\alpha = \beta = \gamma = 90^\circ$	$\frac{(h^2 + k^2 + l^2)}{a^2}$
Tetragonal	$a = b; c$ $\alpha = \beta = \gamma = 90^\circ$	$\frac{(h^2 + k^2)}{a^2} + \frac{l^2}{c^2}$
Orthorhombic	$a; b; c$ $\alpha = \beta = \gamma = 90^\circ$	$\frac{h^2}{a^2} + \frac{k^2}{b^2} + \frac{l^2}{c^2}$
Hexagonal	$a = b; c$ $\alpha = \beta = 90^\circ; \gamma = 120^\circ$	$\frac{(h^2 + hk + k^2)}{a^2 \sin^2 120^\circ} + \frac{l^2}{c^2}$
Rhombohedral	$a = b = c$ $\alpha = \beta = \gamma$	$\frac{[(h^2 + k^2 + l^2) \sin^2 \alpha + 2(kl + hl + hk)(\cos^2 \alpha - \cos \alpha)]}{a^2(1 - 3 \cos^2 \alpha + 2 \cos^3 \alpha)}$
Monoclinic	$a; b; c$ $\alpha = \gamma = 90^\circ; \beta$	$\frac{h^2}{a^2 \sin^2 \beta} + \frac{k^2}{b^2} + \frac{l^2}{c^2 \sin^2 \beta} - \frac{2hl \cos \beta}{ac \sin^2 \beta}$
Triclinic	$a; b; c$ $\alpha; \beta; \gamma$	$\frac{1}{4\pi^2} [h^2 a^{*2} + k^2 b^{*2} + l^2 c^{*2} + 2(klb^* c^* \cos \alpha^* + hla^* c^* \cos \beta^* + hka^* b^* \cos \gamma^*)]$

Analysis of the peak locations in powder diffraction patterns involves searching for algebraic relationships between the scattering angles of the observed diffraction maxima and possible unit cell structures, i.e., lengths  $a, b, c$  and angles  $\alpha, \beta, \gamma$ . Generally, as the crystal class decreases in symmetry, there are more unit cell parameters that need to be determined from the pattern (from one in the cubic system to six in the triclinic system); likewise, the pattern becomes more complicated with increasing numbers of diffraction peaks.<sup>10</sup> Sometimes, two or more different sets of reflections can create additional multiplicities that also contribute to observed intensities.

<sup>10</sup> *J. Appl. Cryst.* **1972**, 5, 271; **1985**, 18, 367.

For example, for a cubic cell, the sets of reflections  $(hkl) = (411)$  and  $(330)$  both have the same  $d$ -spacings, i.e.,  $d_{411} = d_{330}$ .

The peak shapes also provide useful information about the nature of the polycrystalline specimen. Under ideal conditions, peak widths can assess crystallite (particle) sizes via the Scherrer equation, which shows that crystallite size varies inversely with peak width. For a given peak indexed as  $(hkl)$ , the crystallite size in the direction normal to the  $(hkl)$  plane is

$$D_{hkl} = \frac{\kappa\lambda}{\beta_{hkl} \cos \theta_{hkl}}.$$

The peak's full width at half maximum (radians) must be corrected for instrumental broadening, which can be evaluated by inserting a standard sample.  $\kappa$  is a shape parameter, that varies from  $\sim 0.6$ – $2.1$  and is  $0.94$  for a spherical crystal with cubic symmetry.<sup>11</sup>

**(30)** In a powder pattern, every diffraction peak must be indexed  $(hkl)$  to obtain lattice parameters for the unit cell. This indexing requires assessment of the crystal class, and it is not always possible to achieve this, although statistical techniques in data fitting provide increasing success. A powder pattern generally plots relative intensities vs scattering angle  $2\theta$ . Accurate determination of the scattering angles will give  $d$ -spacings between lattice planes in the crystal. According to the Bragg equation, as scattering angle increases,  $d$ -spacings decrease; according to the Ewald sphere restriction, the shortest  $d$ -spacing accessible will be  $\lambda/2$ . Since the largest  $d$ -spacings will lead to low scattering angles, these peaks will generally correspond to unit cell vectors.

As an example, consider the X-ray diffraction pattern for the tetragonal structure of CuAu, space group  $P4/mmm$ , using Cu  $K\alpha$  radiation ( $\lambda = 1.5406 \text{ \AA}$ ). Each peak corresponds to a specific set of  $\{hkl\}$  values. The integrated intensity for a peak  $I_{hkl}$  is related to the product of the multiplicity  $m_{hkl}$ , arising from rotational symmetry, the Lorentz-polarization factor  $LP(2\theta_{hkl})$ , which depends on the scattering angle, and the geometrical structure factor  $S_{hkl}$  of the peak. To demonstrate how powder diffraction helps to identify a phase, we'll use the first four observed peaks in the powder diffraction pattern:

Peak #	$2\theta$	$d_{hkl}$	$hkl$	$m_{hkl}$	$LP_{hkl}$	$S_{hkl}$
1	24.21°	3.673 Å	001	2	21.30	$f_{\text{Au}} - f_{\text{Cu}}$
2	31.89°	2.804 Å	100	4	11.86	$f_{\text{Au}} - f_{\text{Cu}}$
3	40.44°	2.229 Å	101	8	7.05	$f_{\text{Au}} + f_{\text{Cu}}$
4	45.72°	1.983 Å	110	4	5.35	$f_{\text{Au}} + f_{\text{Cu}}$

Standard procedure begins by measuring the  $2\theta$  values for the peaks. Then, use the Bragg equation to evaluate  $d_{hkl}$ . Since the space group or crystal class is often unknown, programs begin by taking ratios of different  $d$ -spacings to search for geometrical relationships that may shed light on the unit cell shape and size, as well as to determine whether the lattice symmetry involves centering, such body- or face-centering, or not. In this example of CuAu, since we know the lattice symmetry is primitive tetragonal, there are two lengths scales of the unit cell ( $a = b$ , and  $c$ ) and no systematic absences among the  $\{hkl\}$  indices. Therefore, the first 4 peaks will have the  $\{hkl\}$  indices:  $(100) = (010)$ ;  $(001)$ ;  $(110) = (\bar{1}10)$ ; and  $(101) = (011) = (\bar{1}01) = (0\bar{1}1)$ , but the order is not yet determined. Since the ratio  $(2.804 \text{ \AA}/1.983 \text{ \AA}) = \sqrt{2}$ , then we may conclude that

<sup>11</sup> *J. Appl. Cryst.* **1978**, *11*, 102-113.

peak #2 is (100) = (010) and peak #4 is (110) = ( $\bar{1}10$ ). Furthermore, peak #1 is (001) and peak #3 is (101) = (011) = ( $\bar{1}01$ ) = (0 $\bar{1}1$ ).

The other aspects of every powder diffraction pattern are the peak intensities. Three important contributions to peak intensities are multiplicity, Lorentz-polarization, and the geometrical structure factor. The multiplicity for each peak, excluding possible accidental superposition, e.g., {330} and {411} peaks for cubic structures, is determined by their rotational equivalences and Friedel's law. The Lorentz-polarization factor depends on the scattering angle  $2\theta_{hkl}$ . Lastly, the geometrical structure factor for the CuAu structure is the sum of two atomic scattering factors:

$$S_{hkl} = f_{\text{Au}} + f_{\text{Cu}}e^{i\pi(h+k+l)} = f_{\text{Au}} + f_{\text{Cu}}(-1)^{h+k+l}.$$

**(31)** Generally, higher crystallographic symmetry leads to a simpler powder diffraction diagram over lower symmetry. As a demonstration of this effect, consider a hypothetical FCC structure of "CuAu" in which the Cu and Au atoms are randomly distributed over the positions of a FCC unit cell. Compare the powder diffraction pattern of this model structure with one with the same unit cell parameters but an ordered arrangement of Au and Cu atoms, and with the pattern for the actual tetragonal structure of CuAu. The pattern for the disordered FCC structure shows fewer positions of constructive interference than that of either tetragonal structure arising from the systematic absences for the *F*-centered lattice. On ordering the atoms, additional reflections become observed. On distortion, peaks shift. Peaks that index with shorter *d*-spacings in real space, i.e., in the crystal, move to higher scattering angles and peaks indexing to longer *d*-spacings in real space move to lower scattering angles. For example, the {200} reflection with multiplicity 6 is a single peak in the X-ray powder pattern of the disordered FCC structure. On ordering of Au and Cu atoms, it remains a single peak because the interatomic distances remain unchanged, but the indices are now {110} and {002} set by the atomic ordering. Lastly, upon distorting the structure to give different unit cell parameters, this peak splits into two distinct ones.

#### Advances in Diffraction Techniques:

Consistent improvements in X-ray detection continue to provide more data that can be collected and analyzed. These data give information about the short-, intermediate-, and long-range order in complex solids. In particular, parallel detection methods allow access to diffraction/scattering effects between the Bragg peaks. This information can be used to determine the nature of disorder or possible superstructure formation in solids. Improvements in powder diffraction instrumentation enhance the effectiveness of pair-distribution functions for analyzing long- and short-range order in solids.

**(32) Diffuse Scattering:** If there is disorder in a sample, any diffraction measurement will exhibit some background that is called diffuse scattering. This type of scattering can show different behavior depending upon the type of disorder creating it, so careful analysis of regions between Bragg peaks can help address problems that may arise during structure refinements. Types of disorder include (1) thermal; (2) occupational; (3) displacement; and (4) stacking faults. The scattering amplitude  $F(\mathbf{h})$ , involving disorder, can be expressed ( $hkl \equiv \mathbf{h}$ ):

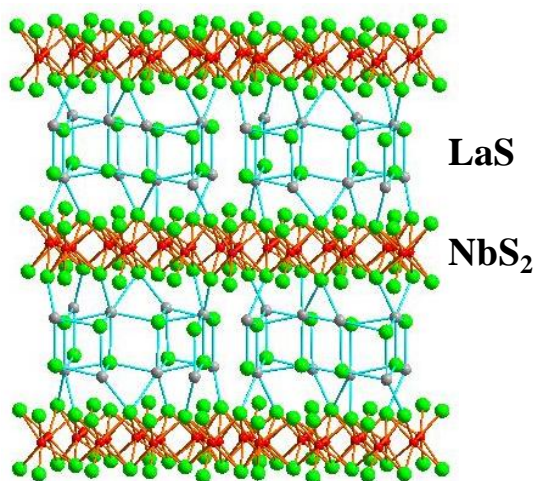
$$F(\mathbf{h}) = \sum \langle f \rangle e^{2\pi i \mathbf{h} \cdot \langle \mathbf{u} \rangle} + \sum (f - \langle f \rangle) e^{2\pi i \mathbf{h} \cdot \langle \mathbf{u} \rangle} + \sum \langle f \rangle e^{2\pi i \mathbf{h} \cdot (\mathbf{u} - \langle \mathbf{u} \rangle)} + \sum (f - \langle f \rangle) e^{2\pi i \mathbf{h} \cdot (\mathbf{u} - \langle \mathbf{u} \rangle)}.$$

In this expression,  $\langle f \rangle$  is the average atomic scattering factor and  $\langle \mathbf{u} \rangle$  is the average position of the atom. The first term is the normal Bragg reflection arising from constructive interference of all scattered waves; the other three terms contribute to diffuse scattering. Term 2 contributes from occupational disorder, which can mean randomly arranged vacancies or mixed site occupancies by two atoms; term 3 contributes from displacement and thermal disorder; and term 4 arises from

a combination of the two. For thermal/displacement disorder effects, the intensity from diffuse scattering is largest for large values of  $\mathbf{h}$ : since  $\mathbf{u} - \langle \mathbf{u} \rangle$  is small, then  $\mathbf{h} \cdot (\mathbf{u} - \langle \mathbf{u} \rangle)$  is small for small  $\mathbf{h}$  so that there is practically no phase change, but  $\mathbf{h} \cdot (\mathbf{u} - \langle \mathbf{u} \rangle)$  becomes significant for large  $\mathbf{h}$ . For occupational disorder, the intensity from diffuse scattering is largest for small  $\mathbf{h}$ , due to the relationship between the atomic scattering factor and  $\mathbf{h}$ .

**(33)** Stacking faults are a form of occupational and displacement disorder arising from irregular stacking sequences. A comparison between CCP and HCP structures, both of which give discrete diffraction patterns for quasi-infinite domains, with a randomly disordered HCP/CCP stackings shows that diffuse scattering in the form of streaks occurs parallel to the stacking direction. There is no streaking observed in planes perpendicular to the stacking direction, an observation that indicates long-range order within each close packed plane.

**(34)** *Aperiodic Structures:* Many solids form periodic structures that are assigned to one of the 230 3-d space groups. However, advances in diffraction technology have uncovered numerous structures that are aperiodic, quasi-periodic, or almost periodic, i.e., structures for which these traditional space groups cannot describe their long-range order. Aperiodic structures include modulated structures, composite structures, and quasicrystals. Modulations in site composition or position can be either commensurate or incommensurate with respect to an underlying crystalline lattice. Also, ordering of magnetic moments assigned to atoms with unpaired electron spins, an effect that can be observed by neutron diffraction, can be commensurate or incommensurate with structural periodicity. Composite structures involve the combination of two distinct components which repeat in space either in phase or out of phase with each other. Some composite structures are called “misfit” layered structures<sup>12</sup> because they consist of two distinct layers with lattice spacings that do not quite match, e.g.,  $(\text{LaS})_{1.14}(\text{NbS}_2)^{13}$  shown here. Lastly, quasicrystals show diffraction patterns with non-crystallographic rotation symmetry, such as 10-fold or icosahedral symmetry.



**(35)** *Modulated structures:* If a solid-state structure contains at least two types of atoms that show two different translational periodicities, the diffraction experiment will reveal these different periodicities. If the two periodicities are related by a rational number, then there will be *satellite* reflections surrounding main reflections for the primary scatterers. Analysis of just the main reflections will give an averaged electron density for the atoms showing the other periodicity. If, however, the two periodicities are related by an *irrational number*, then an additional wavevector must be included to account for this translational symmetry. This approach is called 3+1-*dimensional* crystallography and leads to the concept of *super-space groups*.

The super-space formalism has been introduced to describe various aperiodic crystals. As mentioned above, a modulated crystal structure differs from a regular periodic structure by the presence of additional satellite reflections in its diffraction pattern. These additional spots, which

<sup>12</sup> N. Ng, T.M. McQueen, *APL Mater.* **2022**, *10*, 100901.

<sup>13</sup> A. Meerschaut, P. Rabu, J. Rouxel P. Monceau, A. Smontara, *Mater. Res. Bull.* **1990**, *25*, 855; G.A. Wiegers, R.J. Haange, *J.Phys.: Condens. Matter* **1990**, *2*, 455.

tend to surround the primary spots, indicate that a hypothetical *basic arrangement* adopting one of the 230 3-d space group symmetries has been periodically deformed. If the periodicity of these additional spots is some rational fraction of the primary spots, then a commensurately modulated structure, or *superstructure*, arises. Such a crystal also conforms to one of the 230 space groups. On the other hand, if the periodicity of the modulation is not a rational fraction of the periodicities of the basic structure, then an incommensurately modulated structure results, and the typical space groups are insufficient. These modulations can originate from displacements of the atoms about equilibrium positions, called *displacive modulation*, as well as deformations of the atomic probability functions, called *occupation modulation*. Although an incommensurately modulated structure presents no 3-d translational symmetry, it is not disordered as shown in ideal cases by the presence of sharp, well separated diffraction spots.

For such modulated structures, the scattering vectors in the Fourier expansion of the electron density, i.e., the main reflections and satellites, are expressed as an integral linear combination of  $3+n$  independent basis vectors. In  $(3+n)$ -dimensional crystallography, an atom's position is described by an average position plus a set of  $n$  periodic atomic modulation functions, often introduced as a Fourier series. The atomic occupations and Debye-Waller factors can also be modulated. All the concepts used in normal 3-d crystallography, viz., lattice, unit cell, point group, space group, etc., have been extended to  $(3+n)$ -dimensional crystallography. In the 3-d case, a structure is fully described by giving the lattice and the atomic motif within the unit cell. In a similar way, in an incommensurate  $(3+n)$ -d case, a structure is fully described by giving the metrics (lattice parameters and  $\mathbf{q}$  vectors) and the atom descriptions (type, position, occupancy, Debye-Waller factors, and modulation functions for each parameter). A 3-d crystal structure without translations can be recovered by looking at a given hyper-plane, which is a 3-d section of the  $(3+n)$ -d periodic space. However, it is worth noticing that all structural information is contained within one unit cell of the super-space. For a complete description of the concepts and notations used for incommensurately modulated structures, see the following references:

- T. Janssen, A. Janner, A. Looijenga-Vos, P.M. de Wolff, *International Tables for X-ray Crystallography*, Vol. C, Ch.9.8, 1993.
- De Wolff, P. M. *Acta Cryst.* **1974**, A30, 777-785.
- van Smaalen, S. *Crystallogr. Rev.* **1995**, 4, 79-202.

**(36)** An example of a modulated structure is rhombohedral  $\text{Sr}_{9/8}\text{TiS}_3$ ,<sup>14</sup> which is an example of a hexagonal perovskite and reveals two subsystems with two different periodicities along just the  $c$ -axis: (1) the Sr atoms and (2) chains of trans face-sharing  $\text{TiS}_{6/2}$  octahedra. Satellites in the diffraction pattern along the  $c^*$  axis, reflections that were indexed as  $l = 9, 16, 18$  in particular, were used to identify and solve this modulated structure. Layers of Sr atoms repeat quasi-periodically every 5.305 Å;  $\text{TiS}_{6/2}$  octahedra repeat every 2.984 Å. The super-space group symbol for this structure is reported to be  $R\bar{3}m(00\gamma)0s$ ; the piece in parentheses indicates the direction of the  $q$  vector followed by a piece that identifies intrinsic shifts along the additional axes. The corresponding unit cell is  $a = 11.482$  Å,  $c = 2.9843$  Å, with  $q = 0.5625 c^*$ . The structure can be refined using a conventional space group:  $R\bar{3}c$  with  $a = 11.482$  Å,  $c = 47.749$  Å. However, the (001) reflection using Cu  $K\alpha$  radiation would occur for  $2\theta \sim 1.8^\circ$ .

<sup>14</sup> O. Gourdon, et al. *Acta Cryst.* **2000**, B56, 409-418.

**(37) Pair Distribution Functions:**<sup>15</sup> The intensities and positions of Bragg reflections only allow determination of the long-range *average structure* of a crystal. Any deviations from the average structure result in the occurrence of diffuse scattering, which contains information about two-body interactions. One method to reveal *local* structural features within a crystal is analysis of the *pair distribution function*, PDF. This analysis is long known in the field of studying short-range order in liquids and glasses but has recently been applied to crystalline materials. The PDF is obtained from the powder diffraction data by Fourier transforming the normalized scattering intensity  $S(q)$ :

$$G(r) = 4\pi r[\rho(r) - \rho_0] = \frac{2}{\pi} \int_0^\infty q[S(q) - 1] \sin(qr) dq$$

$\rho(r)$  is the microscopic pair density,  $\rho_0$  is the average number density, and  $q$  is the magnitude of the scattering vector for elastic scattering, i.e.,  $q = 4\pi \sin \theta / \lambda$ .

Since the PDF contains both Bragg and diffuse scattering, information about *local* arrangements is preserved. The PDF can be understood as a bond-length distribution, up to some maximum distance, between all atom pairs  $i$  and  $j$  within the crystal. Moreover, each contribution has a weight corresponding to the scattering power of the two atoms involved. As such, the PDF is the powder diffraction analogue of the Patterson function in single crystal diffraction. The PDF of a given structure can be calculated using the relation:

$$G_{\text{calc}}(r) = \frac{1}{r} \sum_i \sum_j \left[ \frac{b_i b_j}{\langle b \rangle^2} \delta(r - r_{ij}) \right] - 4\pi r \rho_0.$$

The summation goes over all atom pairs within the model crystal separated by  $r_{ij}$ . The scattering power of atom  $i$  is  $b_i$  and  $\langle b \rangle$  is the average scattering power of the sample. For neutron scattering,  $b_i$  is the scattering length; for X-ray scattering, it is the atomic scattering factor evaluated at a user defined value of  $q$ . The default value is  $q = 0$  at which  $b_i$  is the number of electrons  $Z_i$ .

There are two different ways, in general, to account for displacements (either thermal or static) from the average positions. First, one can use a large enough model containing the desired displacements and perform an ensemble average. This is the method used by the *DISCUS* Simulation Package,<sup>16</sup> in which thermal displacements can be introduced according to a given, isotropic Debye-Waller factor. Secondly, one can convolute each contribution given by  $\delta(r - r_{ij})$  in the equation above with a Gaussian function to account for the displacements, a procedure that is done e.g. in the program *PDFFIT*.<sup>17</sup>

To carry out a proper Fourier transform to calculate  $G(r)$ , we would need to measure data up to  $q = \infty$ , which, of course, is not possible. Thus, the termination at a value of  $q = q_{\text{max}}$  will cause so-called *termination ripples* in the PDF. These features can be simulated by convoluting the calculated PDF with the Fourier transform of a box function. With the availability of modern synchrotron and neutron sources, it is possible to collect powder diffraction data up to high values in  $q$ ; however, in many cases a sufficient PDF can be obtained using a conventional X-ray tube. One last correction applied to the calculated PDF,  $G_{\text{calc}}(r)$ , accounts for the limited resolution of the experiment in  $q$ -space. This leads to a decrease of the PDF peak as a function of  $r$  according to the relation  $\exp(-\sigma_q^2 r^2 / 2)$ .

<sup>15</sup> S.J.L. Billinge, *Z. Kristallogr.* **2004**, 219, 117-121.

<sup>16</sup> Th. Proffen and R. B. Neder, *J. Appl. Crystallogr.* **1997**, 30, 171-175; <https://tproffen.github.io/DiffuseCode/>

<sup>17</sup> Th. Proffen and S. J. L. Billinge, *J. Appl. Crystallogr.* **1999**, 32, 572;  
<https://www.xray.cz/ecm-cd/soft/xray/general/discus/discus/pdfit.html>

(38) To obtain a PDF, the raw data, which is collected as counts vs. wavelength or counts vs. scattering angle, is transformed into the normalized scattering intensity vs. scattering length  $Q$ . Then, via Fourier transforms, the PDF vs. distance plot is obtained.

(39) As an example of applying PDF analysis to a diffraction experiment, consider Buckminsterfullerene,  $C_{60}$ , which crystallizes in a face-centered cubic unit cell. These molecules are  $\sim 7.1$  Å in diameter, built up of five- and six-membered rings of 60 C atoms. In the crystal, these molecules freely rotate about their corresponding cage centers, so evaluation of the electron density gives a spherical shell with no *localized* atomic sites. The PDF analysis reveals both short-range, i.e., intramolecular, and intermediate-range, i.e., intermolecular, information.  $G(r)$  shows sharp peaks for the intramolecular contacts of 1.4, 2.2, ... Å, but reveals little structure beyond 7.1 Å.<sup>18</sup>

(40) Another example reveals how PDF analysis of a powder diffraction pattern can give information about domains in complex oxides.  $LaMnO_3$  adopts an orthorhombic crystal structure. The experimentally determined PDF shows short-range M–O contacts that are consistent with Jahn-Teller distortion associated with  $Mn^{3+}$  in octahedral coordination. Intermediate distance correlations give additional information about atom pairs within domains and between domains in the sample.<sup>19</sup>

---

<sup>18</sup> Th. Proffen, et al., *Z. Kristallogr.* **2003**, 218, 132-143.

<sup>19</sup> Proffen et al., *Phys. Rev. B* **1999**, 60, 9973.